Research Square

Preprints are preliminary reports that have not undergone peer review.
They should not be considered conclusive, used to inform clinical practice,
or referenced by the media as validated information.

Interconnected roles of FAM83H, PD-L1, and β-catenin in the progression of ovarian carcinoma

Junyue Zhang
Jeonbuk National University Medical School
Kyoung Min Kim
Jeonbuk National University Medical School
Hyun Sun Kim
Jeonbuk National University Medical School
Won Ku Choi
Jeonbuk National University Medical School
Ae-Ri Ahn
Jeonbuk National University Medical School
Ho Sung Park
Jeonbuk National University Medical School
See-Hyoung Park
Hongik University
Dong Hyu Cho
Jeonbuk National University Medical School
Young Jae Moon
Jeonbuk National University Medical School
Kyu Yun Jang
kyjang@jbnu.ac.kr

Jeonbuk National University Medical School

Research Article

Keywords: Ovarian carcinoma, FAM83H, PD-L1, β-catenin, prognosis, ubiquitination

Posted Date: October 21st, 2026

DOI: https://doi.org/10.21203/rs.3.rs-7828723/v1

License: This work is licensed under a Creative Commons Attribution 4.0 International License.
Read Full License

Additional Declarations: No competing interests reported.

Interconnected roles of FAM83H, PD-L1, and β-catenin in the progression of ovarian carcinoma

Junyue Zhang[1,†], Kyoung Min Kim[2,†], Hyun Sun Kim[2], Won Ku Choi[3], Ae-Ri Ahn[2], Ho Sung Park[2], See-Hyoung Park[4], Dong Hyu Cho[3], Young Jae Moon[1,5,*], Kyu Yun Jang[2,5,*]

[1]Department of Biochemistry and Molecular Biology, Jeonbuk National University Medical School, 54896 Jeonju, Republic of Korea;

[2]Department of Pathology, Jeonbuk National University Medical School, Jeonju 54896, Republic of Korea;

[3]Department of Obstetrics and Gynecology, Jeonbuk National University Medical School, Jeonju 54896, Republic of Korea

[4]Department of Bio and Chemical Engineering, Hongik University, Sejong 30016, Republic of Korea

[5]Research Institute of Clinical Medicine of Jeonbuk National University-Biomedical Research Institute of Jeonbuk National University Hospital, Jeonju 54896, Republic of Korea

[†] These authors contributed equally to this work

[*] Correspondence: kyjang@jbnu.ac.kr, yjmoonos@jbnu.ac.kr

Email addresses:

Junyue Zhang: yuezai123@naver.com; Kyoung Min Kim: kmkim@jbnu.ac.kr; Hyun Sun

Kim: gustjs135@jbnu.ac.kr; Won Ku Choi: wkchoi@jbnu.ac.kr; Ae-Ri Ahn: arahn@jbnu.ac.kr; Ho Sung Park: hspark@jbnu.ac.kr; See-Hyoung Park: shpark74@hongik.ac.kr; Dong Hyu Cho: obgyn2001@jbnu.ac.kr; Young Jae Moon: yjmoonos@jbnu.ac.kr; Kyu Yun Jang: kyjang@jbnu.ac.kr

Abstract

Background

Initial research on FAM83H focused on its role in dental development; subsequent it has been studied based on its role in oncology as it affects various oncogenic pathways. In particular, the possibility of an association between FAM83H and the β-catenin pathway and antitumor immunity has been suggested. However, the specific relationships among FAM83H, PD-L1, and β-catenin have not been evaluated in human cancers, especially in ovarian cancer.

Methods

This study evaluated the interconnected roles of FAM83H, PD-L1, and β-catenin in ovarian carcinomas in 150 human ovarian carcinoma samples and ovarian cancer cells.

Results

Immunohistochemical expression of FAM83H, PD-L1, and β-catenin was significantly associated with each other, and their individual and combined expression patterns were significantly associated with shorter overall survival and relapse-free survival. In ovarian cancer cells, the protein expression of FAM83H, PD-L1, and β-catenin was positively associated with each other; however a corresponding association with the mRNA expression of these genes was not found. Direct binding between FAM83H, PD-L1, and β-catenin was predicted via molecular docking analysis *via* protein sequences. In addition, immunoprecipitation data revealed that FAM83H, PD-L1, and β-catenin directly bind and form a complex. Furthermore, knockdown of FAM83H accelerated the ubiquitination and proteasomal degradation of PD-L1 and β-catenin. Knockdown of PD-L1 increased the

ubiquitination of FAM83H and β-catenin, and knockdown of β-catenin increased the ubiquitination of FAM83H and PD-L1. *In an in vivo* tumor model in C57BL/6J mice, overexpression of FAM83H was associated with increased infiltration of FOXP3-positive regulatory T cells and PD-1-positive lymphoid cells and decreased infiltration of CD8-positive cytotoxic T cells, and *vice versa,* with knockdown of FAM83H.

Conclusions

This study revealed that the individual and combined expression patterns of FAM83H, PD-L1, and β-catenin might be used as prognostic indicators of ovarian carcinoma. Furthermore, FAM83H, PD-L1, and β-catenin form a complex and stabilize each other, and are associated with the proliferation of ovarian cancer cells and the regulation of peritumoral immune cell infiltration. Therefore, the interactions between FAM83H, PD-L1, and β-catenin might be a potential therapeutic targets for ovarian carcinomas.

Keywords

Ovarian carcinoma, FAM83H, PD-L1, β-catenin, prognosis, ubiquitination

Background

The family with sequence similarity 83 H (FAM83H) is a member of the FAM83 family and it plays an important role in tooth development through its involvement in dental enamel formation [1, 2]. Furthermore, FAM83H has more recently been of interest because of its role in the organization of the keratin cytoskeleton in human cancers [3]. Higher expression of FAM83H in human cancers than in nonneoplastic tissue has been reported [4, 5]. Higher expression of FAM83H is also associated with cancer progression and poor prognosis in cancer patients [4, 6-8]. During cancer development and progression, FAM83H stimulates cellular proliferation, invasiveness, and resistance to anticancer therapy by affecting signaling related to apoptosis, cell cycle progression, epithelial-to-mesenchymal transition (EMT), and immune evasion [6-8]. During these processes, FAM83H affects cancer progression in conjunction with other molecules, especially β-catenin [7, 8].

As a hallmark of cancer progression, understanding immune evasion of cancer cells is critical in the clinical field of cancer therapy [9]. In particular, CTLA4- and PD-L1/PD1-mediated escape of cancer cells from immune surveillance is a focus of clinical anticancer therapies which target these pathways; furthermore the unexpected failure of therapies in some populations of cancer patients has been attributed to CTLA4- or PD-L1/PD1-mediated escape from immune surveillance [9, 10]. Therefore, a precise understanding of the mechanism of cancer immune evasion and the therapies targeted to overcome the present limitations of immune checkpoint inhibitors is needed [10]. Immune checkpoint inhibitors targeting PD-L1, PD-L1 expression is regulated in conjunction with other molecules [11] and

higher expression of PD-L1 is associated with shorter survival of cancer patients, and higher expression of PD-L1 is used to select cancer patients for anti-PD-L1/PD1 therapies [12]. In this context, maintaining PD-L1 expression in cancer cells might be important in the immune evasion of cancer cells. Therefore, understanding the mechanism related to the expression and stabilization of PD-L1 is important for the success of PD-L1/PD1-targeted therapy.

The canonical Wnt/β-catenin pathway is a highly conserved signaling pathway that plays an important role in the regulation of cellular proliferation and maintaining homeostasis [13, 14]. However, its expression is tightly controlled by the destruction of β-catenin through proteasomal degradation [13, 14]. In a nonphysiological state, especially in cancer, β-catenin escapes proteasomal degradation by interfering with destruction complex formation-mediated degradation [13, 14]. This causes β-catenin to accumulate in the cytoplasm and translocate to the nucleus, where it activates the transcription of oncogenic target genes [13, 14]. With respect to the stabilization of β-catenin, FAM83H stabilizes β-catenin from proteasomal degradation and stimulates the proliferation and invasiveness of cancer cells [7, 8]. Furthermore, FAM83H has been suggested to be associated with anticancer immune environments [15, 16] and β-catenin induces and stabilizes PD-L1 in human cancers [13, 17]. Therefore, there might be an association between FAM83H, PD-L1, and β-catenin in cancer progression.

Ovarian cancer is the eighth most common cancer diagnosed in women and the fifth most common cause of cancer death in women [18]. Despite advances in anticancer therapy, however, ovarian cancer still has a high mortality rate, and the 5-year relative survival rate remains at 51% [18]. Even recently developed immune checkpoint inhibitors have shown

limited efficacy in treating ovarian cancer when used as monotherapies [19]. However, when the efficacy of a combination of PD-L1/PD1 inhibitors with chemotherapeutic agents or dual checkpoint inhibition in ovarian cancer therapy is considered, a study investigating the multiple aspects of cancer hallmarks might serve to improve anticancer treatment strategies [19]. In this context, it has been suggested that FAM83H is associated with cancer progression through its affects host immunity and its ability to regulate the stabilization of β-catenin [7, 8, 15, 16]. Furthermore, β-catenin is involved in cancer progression and resistance to therapy by inducing PD-L1 expression and stimulating cancer-associated signaling [13, 14]. Therefore, considering the role of PD-L1 in the immune evasion of cancer cells [20] and the roles of FAM83H and β-catenin in the progression of human cancers [6-8, 13], these three molecules might play interconnected roles in cancer progression. However, studies focused on the relationships between these molecules are lacking, especially in patients with ovarian cancer. Therefore, this study evaluated the interconnected roles of FAM83H, PD-L1, and β-catenin in ovarian carcinomas in human ovarian carcinomas and cells.

Methods

Ovarian carcinomas and immunohistochemical staining

This study evaluated 150 ovarian carcinoma patients who underwent an operation between January 1996 and December 2012. Patients whose complete medical records and histologic slides and tissue blocks were available were included in this study. Clinicopathological information was obtained from medical records. Histology and cancer stage were reviewed

according to the 5th edition of the World Health Organization classification of ovarian tumors [21] and the 8th edition of the American Joint Committee on Cancer staging system [22]. The histologic subtypes of ovarian carcinoma included in this study were 21 low-grade serous carcinomas, 77 high-grade serous carcinomas, 34 mucinous carcinomas, 11 endometrioid carcinomas, 5 clear cell carcinomas, and 2 malignant Brenner tumors. Postoperatively, 118 patients received platinum- and taxoid-based adjuvant chemotherapy, and platinum resistance was evaluated according to standard Gynecologic Oncology Group criteria [23]. This study was approved by the institutional review board of Jeonbuk National University Hospital (IRB number, CUH 2025-05-004; approval date, May 14, 2025) and was performed according to the Declaration of Helsinki. Written informed consent was waived during approval of the IRB on the basis of the retrospective and anonymous character of the study.

Immunohistochemical staining for FAM83H, PD-L1, and β-catenin was performed in human tissue samples using 3.0 mm core tissue microarray (TMA) sections. Two TMA cores were arrayed in each case from the original tissue blocks. The tissue sections were immunostained with anti-FAM83H (#A304-328A, 1:100, Bethyl Laboratories, Montgomery, TX, USA), anti-PD-L1 (#13684, 1:100, Cell Signaling Technology, Beverly, MA, USA), and anti-β-catenin (# 610154, 1:100, BD Biosciences, Milpitas, CA, USA) antibodies after deparaffinization and antigen retrieval by boiling in a microwave oven with pH 6.0 antigen retrieval solution (DAKO, Glostrup, Denmark) for 20 minutes. Immunostained slides were scored by adding the staining intensity (0, no staining; 1, weak; 2, intermediate; 3, strong) and staining area point (0, no staining; 1, 1%; 2, 2-10%; 3, 11-33%; 4, 34-66%; 5, 67-100%) [15, 24, 25]. The score obtained from each TMA core from the two TMA cores per case was

added and used as the final immunohistochemical staining score, ranging from zero to sixteen.

Bioinformatic analysis and use of public databases

In this study, we searched the GEPIA public database (http://gepia.cancer-pku.cn, accessed on 1 August 2025) and the Gene Expression Omnibus (GEO, https://www.ncbi.nlm.nih.gov/geo, accessed on 1 August 2025) database. The GEO database was used to identify transcriptomic alterations associated with different stages and conditions of human ovarian cancers. From the datasets updated within the past decade in the GEO database, we retrieved datasets representing key aspects of ovarian cancer progression: genes significantly increased in high-grade serous ovarian carcinomas compared with normal tissue (*GSE223426*); genes significantly increased in metastatic ovarian cancer lesions compared with primary ovarian cancers (*GSE178913*); genes significantly increased in platinum-resistant ovarian cancers compared with platinum-sensitive ovarian cancers (*GSE98230*); and genes significantly increased in serous ovarian carcinomas compared with serous ovarian borderline tumors (*GSE36668*). Differential gene expression analysis was performed using the *DESeq2* package in R (version 4.3.2, https://www.r-project.org). Genes with an absolute $\log_2$ fold change greater than 1 and *P*-values less than 0.05 were considered significantly differentially expressed. Overlaps between datasets were visualized using the *VennDiagram* package in R.

Molecular docking analysis

The protein structures of FAM83H, PD-L1, and β-catenin were obtained from the UniProt

(https://www.uniprot.org, accessed 10 September 2024) database [26]. PyMOL (version 2.1, Schrödinger, Inc., New York, NY, USA) was used to process these protein structures, which were then uploaded to the HDOCK SERVER website (http://hdock.phys.hust.edu.cn) for protein-protein virtual docking [27]. This experiment selected the combination with the lowest docking score and highest confidence score for simulating the docking site, and PyMOL was used to visualize docking between target proteins.

Cells and transfection

SKOV3 and OVCAR3 ovarian cancer cells were used in this study. OVCAR3 cells were purchased from the Korean Cell Line Bank (KCLB, Seoul, Republic of Korea), and SKOV3 cells were purchased from the American Type Culture Collection (ATCC, Manassas, VA, USA) between 2017 and 2018 and verified by deoxyribonucleic acid fingerprinting analysis from the Korean Cell Line Bank (KCLB, Seoul, Republic of Korea). The OVCAR3 cell line was cultured in RPMI 1640 culture medium, and the SKOV3 cell line was cultured in Dulbecco's Modified Eagle's Medium (DMEM)/F12 culture medium. The culture media contained 10% fetal bovine serum (Gibco BRL, Gaithersburg, MD, USA) and 1% penicillin/streptomycin (Gibco BRL) and was maintained at 37 °C under humidified conditions with 5% CO_2. The vectors for FAM83H-specific shRNA (#sc-77451-SH, Santa Cruz Biotechnology, Santa Cruz, CA, USA), PD-L1-specific shRNA (#sc-39699-SH, Santa Cruz Biotechnology, Santa Cruz, CA, USA), and β-catenin-specific shRNA (#sc-29209-SH, Santa Cruz Biotechnology, Santa Cruz, CA, USA) were purchased from Santa Cruz Biotechnology (Santa Cruz, CA, USA). The overexpression of FAM83H was induced *via* the

transfection of wild-type FAM83H (#RC219064, Myc-tagged, OriGene Technologies, Rockville, MD, USA). Lipofectamine 3000 (Invitrogen, Carlsbad, CA, USA) was used for cell transfection. The cells transfected with vectors were used in experiments 24 hours after transfection.

Cell Proliferation Assay

A 3-(4, 5-dimethylthiazol-2-yl)-2, 5-diphenyltetrazolium bromide (MTT) cell proliferation assay (Sigma, Saint Louis, MO, USA) and a colony-forming assay were used to evaluate cellular proliferation. For the MTT assay, 2×10^3 SKOV3 cells were seeded in 96-well cell culture plates, and the optical density was measured at a wavelength of 560 nm. For the colony-forming assay, 2×10^3 SKOV3 cells were seeded in 6-well plates and grown for seven days. The colonies on the culture plates were stained with 0.01% crystal violet. Their colony-forming ability was evaluated by measuring the number of colonies with ImageJ software (version 1.54p, https://imagej.net/ij, accessed on 17 February 2025).

Western blotting, immunoprecipitation, and ubiquitination analysis

The total protein of the cultured ovarian carcinoma cells was obtained by lysing the cells with PRO-PREP protein extraction solution (iNtRON Biotechnology, Seongnam, Republic of Korea). The following primary antibodies were used in this study: FAM83H (#A304-328A, Bethyl Laboratories, Montgomery, TX, USA), PD-L1 (#13684, Cell Signaling Technology, Beverly, MA, USA), β-catenin (# 610154, BD Biosciences, Milpitas, CA, USA), actin (#sc-130065, Santa Cruz Biotechnology, Santa Cruz, CA, USA), and glyceraldehyde 3-phosphate

dehydrogenase (GAPDH) (#2118, Cell Signaling Technology, Beverly, MA, USA). For immunoprecipitation, 400 μg of SKOV3 or OVCAR3 protein lysates were immunoprecipitated with anti-FAM83H (Bethyl Laboratories, Montgomery, Texas, USA), anti-β-catenin (BD Biosciences, Milpitas, California, USA), or anti-PD-L1 (Cell Signaling Technology, Beverly, MA, USA) antibodies at 4 °C overnight. The immunocomplexes were pulled down using protein A/G agarose beads (#20421, Thermo Fisher Scientific, Waltham, MA, USA) and the eluted proteins were immunoblotted with anti-FAM83H (Bethyl Laboratories, Montgomery, Texas, USA), anti-β-catenin (BD Biosciences, Milpitas, California, USA), anti-PD-L1 (Cell Signaling Technology, Beverly, MA, USA), and GAPDH antibodies (Cell Signaling Technology, Beverly, MA, USA). For ubiquitin proteasomal degradation and ubiquitination analysis, SKOV3 cells were transfected with a control vector of shRNA or shRNA for FAM83H and treated with 30 μmol/L cycloheximide (CHX, Sigma, Saint Louis, MO, USA) or 30 μmol/L MG132 (Sigma, Saint Louis, MO, USA) for 0.5 to 2.0 hours. The protein lysates were immunoblotted with antibodies against PD-L1 (Cell Signaling Technology, Beverly, MA, USA), β-catenin (BD Biosciences, Milpitas, California, USA), and GAPDH (Cell Signaling Technology, Beverly, MA, USA). In addition, to evaluate the ubiquitination of FAM83H, PD-L1, or β-catenin with the knockdown of FAM83H, PD-L1, or β-catenin, SKOV3 cells were transfected with a control vector of shRNA or shRNA for the indicated target (FAM83H, PD-L1, or β-catenin), and the cells were treated with 30 μmol/L MG132 for two hours. The total cell lysates were immunoprecipitated with anti-PD-L1 (Cell Signaling Technology, Beverly, MA, USA), anti-β-catenin (BD Biosciences, Milpitas, California, USA), or anti- FAM83H (Bethyl Laboratories, Montgomery, Texas,

USA) antibodies, and the eluted proteins were immunoblotted with anti-ubiquitin antibodies (#58395, Cell Signaling Technology, Beverly, MA, USA). The membranes were developed by using an enhanced chemiluminescence detection system (Amersham Biosciences, Buckinghamshire, UK), and images were acquired with a luminescent image analyzer (LAS-4000, Fuji Film, Tokyo, Japan).

Quantitative reverse-transcription polymerase chain reaction

Total RNA was extracted with TRIzol reagent (Invitrogen, Carlsbad, CA, USA) according to the manufacturer's instructions. Reverse transcription to generate cDNA was performed using random hexamer primers from first-strand cDNA synthesis kits (Applied Biosystems, Foster City, CA, USA). A quantitative polymerase chain reaction was performed on 384-well plates using an ABI Prism 7900HT Sequence Detection System (Applied Biosystems, Foster City, CA, USA). The values were normalized to the expression of the GAPDH reference gene. All the experiments were performed in triplicate. The sequences of primers used in the reverse-transcription polymerase chain reaction are listed in Supplementary Table S1.

***In vivo* tumor assay**

The use of mice was approved by the Institutional Animal Care and Use Committee of Jeonbuk National University (IRB number, JBNU NON2025-073-001; approval date, June 12, 2025). To evaluate the effect of FAM83H on tumor growth in conjunction with host immunity in these mice, we evaluated in vivo tumors derived from SKOV3 cells in female C57BL/6J mice (Orient Bio, Seongnam, Republic of Korea), which maintain host immunity.

In accordance with previously described methods [25], SKOV3 cells were transfected with empty vectors, vectors for wild-type FAM83H, or shRNA for FAM83H, and then injected subcutaneously into 4-week-old female BALB/c nude mice (Orient Bio, Seongnam, Republic of Korea) to induce tumor formation. Four mice were included in each group. Tumor volume was measured weekly using the formula "length × width × height × 0.52" to evaluate tumor growth. The mice were euthanized by CO_2 inhalation under sodium pentobarbital anesthesia at six weeks after tumor implantation, just before the largest tumor volume reached 2 cm^3. To evaluate immune cell infiltration around the tumor according to the expression of FAM83H, 2 × 2 × 2 mm^3-sized tumor cubes were implanted subcutaneously into four-week-old female C57BL/6J mice. Four C57BL/6J mice in each group were implanted with tumor cubes, maintained for four days, and euthanized by CO_2 inhalation under sodium pentobarbital anesthesia. Thereafter, tissue sections were obtained to evaluate immune cell infiltration at the edge of the implanted tumor. The resected tumor and surrounding tissues were fixed in neutral formalin, embedded in paraffin, and used for hematoxylin and eosin staining and immunofluorescence staining.

Immunofluorescence staining

SKOV3 and OVCAR3 cells were fixed with 4% formaldehyde. The formalin-fixed and paraffin-embedded tissue sections were deparaffinized, and antigen retrieval performed. The cells and tissue sections were incubated with antibodies against FAM83H (#A304-328A, 1:100, Bethyl Laboratories, Montgomery, TX, USA), FAM83H (#NBP2-32219AF647, 1:100, Novus Biologicals, Centennial, CO, USA), PD-L1 (#13684, 1:200, Cell Signaling

Technology, Beverly, MA, USA), PD-L1 (#29122, 1:200, Cell Signaling Technology, Beverly, MA, USA), β-catenin (# 610154, 1:100, BD Biosciences, Milpitas, California, USA), PD1 (#84651, 1:200, Cell Signaling Technology, Beverly, MA, USA), FOXP3 (#126402, 1:200, BioLegend, San Diego, CA, USA), CD4 (#sc20079, 1:100, Santa Cruz Biotechnology, Santa Cruz, CA, USA), and CD8 (#sc-18860, 1:100, Santa Cruz Biotechnology, Santa Cruz, CA, USA) overnight at 4 °C. The following secondary antibodies were subsequently used: Alexa Fluor 488 anti-mouse IgG (#A-10680, Invitrogen, Carlsbad, CA, USA), Alexa Fluor 594 anti-rabbit IgG (#A-11012, Invitrogen, Carlsbad, CA, USA), Alexa Fluor 488 anti-mouse IgG1 (#A-21121, Invitrogen, Carlsbad, CA, USA), Alexa Fluor 594 anti-mouse IgG2b (#A-21145, Invitrogen, Carlsbad, CA, USA), Alexa Fluor 488 anti-rat IgG2b (#53-4031-80, Invitrogen, Carlsbad, CA, USA), Alexa Fluor 594 anti-mouse IgG (#A-11005, Invitrogen, Carlsbad, CA, USA), and Alexa Fluor 647 anti-rabbit IgG (#A-21244, Invitrogen, Carlsbad, CA, USA). The slides were counterstained with DAPI. Images of the immunofluorescence staining were taken with an APEXVIEW™ APX100 All-in-One Microscope (APX100, Olympus, Tokyo, Japan). The number of positively stained cells was counted in three high-power fields in each case, and the sum of the numbers was used for evaluation. The area of one high-power field image was 0.00367 mm^2. Therefore, 0.01101 mm^2 was evaluated in each case.

Statistical analysis

Positivity of immunohistochemical staining in human ovarian carcinoma tissue was determined by receiver operating characteristic curve analysis at the point with the highest

predictive immunohistochemical score for cancer-related death in patients [28]. Survival analysis was performed for overall survival (OS) and relapse-free survival (RFS) at the endpoint of December 2016. The event of the OS analysis was the cancer-related death of a patient, and the event of the RFS analysis was any relapse of cancer or cancer-related death of a patient. The duration was determined from the date of the operation to the date of the event or the end of follow-up. The prognosis of patients was evaluated with univariate and multivariate Cox proportional hazards regression analyses and Kaplan–Meier survival analysis. The relationships between factors were analyzed with Pearson's chi-square test, and comparisons of the means between groups were analyzed with the Student's *t*-test and ANOVA. All experiments were performed in triplicate, and representative data are presented. Statistical analysis was performed using SPSS software (version 25.0, IBM, Armonk, NY, USA), and *P*-values less than 0.05 were considered statistically significant.

Results

Immunohistochemical expression of FAM83H, PD-L1, and β-catenin were significantly associated with each other and with unfavorable clinicopathological indicators

Human ovarian carcinomas immunohistochemically express FAM83H, PD-L1, and β-catenin (Fig. 1A). The positivity of FAM83H, PD-L1, and β-catenin expression was determined by receiver operating characteristic curve analysis at the point with the highest area under the curve (Fig. 1B). With these cutoff values, FAM83H positivity was significantly associated with age ($P = 0.042$), preoperative serum CA125 level ($P = 0.001$), TNM stage ($P < 0.001$),

histologic type ($P = 0.001$), platinum-resistance ($P = 0.016$), and the expression of PD-L1 ($P < 0.001$) and β-catenin ($P = 0.020$) (Table 1). PD-L1 positivity was significantly associated with serum CA125 level ($P = 0.027$), TNM stage ($P = 0.001$), ascites ($P = 0.043$), bilaterality of the tumor ($P = 0.007$), histologic type ($P < 0.001$), platinum-resistance ($P = 0.006$), and β-catenin expression ($P < 0.001$) (Table 1). β-catenin positivity was significantly associated with tumor size ($P = 0.006$), histologic type ($P = 0.003$), and platinum-resistance ($P = 0.014$) (Table 1).

Immunohistochemical expression of FAM83H, PD-L1, and β-catenin were significantly associated with the survival of ovarian cancer patients

In univariate survival analysis, age (OS; $P < 0.001$, RFS; $P < 0.001$), TNM stage (OS; $P < 0.001$, RFS; $P < 0.001$), lymph node metastasis (OS; $P = 0.031$, RFS; $P = 0.006$), ascites (OS; $P = 0.004$, RFS; $P = 0.007$), bilaterality (OS; $P < 0.001$, RFS; $P < 0.001$), CA125 level (OS; $P < 0.001$, RFS; $P < 0.001$), and the expression of FAM83H (OS; $P < 0.001$, RFS; $P < 0.001$), PD-L1 (OS; $P < 0.001$, RFS; $P < 0.001$), and β-catenin (OS; $P < 0.001$, RFS; $P < 0.002$) were significantly associated with OS and RFS (Table 2). Kaplan-Meier survival analysis revealed that patients with high expression of FAM83H (OS; log-rank $P < 0.001$, RFS; log-rank $P < 0.001$), PD-L1 (OS; log-rank $P < 0.001$, RFS; log-rank $P < 0.001$), and β-catenin (OS; log-rank $P < 0.001$, RFS; log-rank $P = 0.001$) showed shorter survival (Fig. 1C). In addition, when survival analysis was performed according to the histologic subtype of ovarian carcinoma, FAM83H (OS; $P = 0.003$, RFS; $P = 0.013$), PD-L1 (OS; $P = 0.049$, RFS; $P = 0.273$), and β-catenin (OS; $P = 0.006$, RFS; $P = 0.055$) positivity were significantly

associated with shorter OS in high-grade serous carcinoma patients (Fig. 2A). In mucinous carcinomas, FAM83H expression was significantly associated with OS (P = 0.015) and RFS (P = 0.013) and PD-L1 expression was significantly associated with RFS (P = 0.048) (Fig. 2B).

Multivariate analysis was performed with the factors significantly associated with OS and RFS, with the exception of CA125, because 10 patients did not have their preoperative serum levels measured. In multivariate survival analysis, age (OS; P = 0.004, RFS; P = 0.020), TNM stage (OS; P < 0.001, RFS; P < 0.001), FAM83H expression (OS; P = 0.012, RFS; P = 0.008), and β-catenin expression (OS; P = 0.003, RFS; P = 0.030) were independent indicators of OS and RFS (Table 3). FAM38H positivity predicted a 1.924-fold increased risk of death of patients (95% CI [95% confidence interval]: 1.155 - 3.204) and a 1.823-fold increased risk of tumor relapse or patient death (95% CI: 1.172 - 2.837) (Table 3). Positivity of β-catenin was associated with a 2.072-fold increased risk of cancer death (95% CI: 1.281 - 3.352) and a 1.603-fold greater risk of tumor relapse or patient death (95% CI: 1.047 - 2.454) (Table 3).

Furthermore, because of the positive associations among FAM83H, PD-L1, and β-catenin, we evaluated the prognostic significance of the combined expression patterns of FAM83H, PD-L1, and β-catenin. The combined expression patterns were scored according to the number of positive markers from FAM83H, PD-L1, and β-catenin in 150 ovarian carcinomas. The scores were zero (negative for three markers), one (positive for one of three markers), two (positive for two of three markers), or three (positive for three markers). This four-group combined pattern (combined expression Model 1) was significantly associated with OS

(overall $P < 0.001$) and RFS (overall $P = 0.001$) (Fig. 3A). Ovarian cancers with a combined score of zero were associated with the longest survival (5y-OS [OS rate at 5 years] 84%, 10y-OS [OS rate at 10 years] 73%, 5y-RFS [RFS rate at 5 years] 70%, 10y-RFS [RFS rate at 10 years] 59%), and cancers with a combined score of three were associated with the shortest survival (5y-OS 21%, 10y-OS 4%, 5y-RFS 6%, 10y-RFS 0%) (Table 4). The cancers with scores of one (5y-OS 69%, 10y-OS 63%, 5y-RFS 48%, and 10y-RFS 44%) and two (5y-OS 46%, 10y-OS 36%, 5y-RFS 41%, and 10y-RFS 32%) had intermediate survival rates (Table 4). On the basis of the survival rates of these four groups, we further subclassified them into a low-score group (scores of 0 and 1) and a high-score group (scores of 2 and 3), and this model (combined expression Model 2) was significantly associated with OS ($P < 0.001$) and RFS ($P < 0.001$) in 150 patients with ovarian carcinomas (Fig. 3B). When we further analyzed according to histologic subtype, subgrouping was significantly associated with OS ($P = 0.020$) and RFS ($P = 0.025$) in 21 low-grade serous carcinomas (Fig. 3C), OS ($P < 0.001$) in 77 high-grade serous carcinomas (Fig. 3D), and OS ($P = 0.006$) and RFS ($P = 0.002$) in 34 mucinous carcinomas (Fig. 3E).

FAM83H, PD-L1, and β-catenin form a complex and are involved in the stabilization of each other from proteasomal degradation

In our human ovarian carcinomas, FAM83H, PD-L1, and β-catenin expression were associated with the prognosis of ovarian carcinomas. Similarly, in the GEPIA database, the expression of FAM83H was higher in ovarian cancer tissue than in normal tissue (Fig. 4A). In a search of the GEO database, FAM83H was included among 16 genes whose expression

levels significantly increased in four gene expression datasets: higher in high-grade serous carcinoma than in normal tissue, higher in metastatic ovarian cancer than in primary ovarian cancer, higher in platinum-resistant ovarian cancers than in platinum-sensitive cancers, and higher in ovarian serous carcinomas than in borderline serous tumors (Fig. 4B). Because the expression of FAM83H, PD-L1, and β-catenin were significantly associated with cancer progression and resistance, we further evaluated the protein-protein interactions among between FAM83H, PD-L1, and β-catenin *via* molecular docking analysis. As visualized with PyMol software in Figure 4C, there was predicted protein-protein binding between FAM83H and β-catenin (docking score of -334.82, confidence score of 0.9758), FAM83H and PD-L1 (docking score of -293.74, confidence score of 0.9466), and PD-L1 and β-catenin (Docking score of -311.58, confidence score of 0.9620). Furthermore, FAM83H, PD-L1, and β-catenin formed complex binding (docking score of -326.74, confidence score of 0.9427) (Fig. 4C). Information on the amino acids at the docking sites between two proteins is listed in Supplementary Tables S2 and S3.

Therefore, we evaluated the association between FAM83H, PD-L1, and β-catenin in ovarian cancer cells. In SKOV3 and OVCAR3 ovarian cancer cells, the protein expression of PD-L1 and β-catenin increased with the overexpression of FAM83H and decreased with the knockdown of FAM83H (Fig. 4D). However, mRNA expression of PD-L1 and β-catenin was not changed significantly with knockdown or overexpression of FAM83H (Fig. 4D). In addition, PD-L1 knockdown decreased the protein expression of FAM83H and β-catenin but not the mRNA expression of FAM83H or β-catenin (Fig. 4E). Knockdown of β-catenin also decreased the protein expression of FAM83H and PD-L1 but not the mRNA expression of

FAM83H or PD-L1 (Fig. 4F). A positive association between FAM83H, PD-L1, and β-catenin proteins was also evident *via* immunofluorescence staining in ovarian cancer cells after overexpression or knockdown of FAM83H, knockdown of PD-L1, or knockdown of β-catenin (Fig. 4G and 4H).

Furthermore, in support of the results of the molecular docking analysis, immunoblotting after immunoprecipitation of FAM83H, PD-L1, and β-catenin revealed that the proteins FAM83H, PD-L1, and β-catenin directly bind and form a complex (Fig. 5A). However, the positive associations among FAM83H, PD-L1, and β-catenin were detected only at the protein level and not at the mRNA level. These results suggest that FAM83H, PD-L1, and β-catenin are involved in the posttranslational stabilization of each other. Consistent with these findings, knockdown of FAM83H accelerated the proteasomal degradation of PD-L1 and β-catenin (Fig. 5B) and the ubiquitination of PD-L1 and β-catenin in SKOV3 cells (Fig. 5C). Knockdown of PD-L1 increased the ubiquitination of FAM83H and β-catenin (Fig. 5D), and knockdown of β-catenin increased the ubiquitination of FAM83H and PD-L1 (Fig. 5E). These results suggest that FAM83H, PD-L1, and β-catenin are involved in the posttranslational stabilization of each other by forming a complex and suppressing ubiquitin-mediated proteasomal degradation.

FAM83H, PD-L1, and β-catenin are cooperatively involved in the proliferation of ovarian cancer cells, and FAM83H affects the peritumoral infiltration of immune cells

On the basis of the molecular relationships among FAM83H, PD-L1, and β-catenin and their associations with poor prognosis of ovarian carcinoma, we evaluated the effects of their

expression on the proliferation of ovarian cancer cells. We induced PD-L1 and β-catenin knockdown in SKOV3 cells after knocking down or overexpressing FAM83H (Fig. 6A). FAM83H, PD-L1, and β-catenin knockdown significantly inhibited the proliferation of SKOV3 cells according to the MTT and colony formation assays (Fig. 6B and 6C). In addition, co-knockdown of FAM83H and PD-L1 or β-catenin synergistically inhibited the proliferation of SKOV3 cells (Fig. 6B and 6C). Overexpression of FAM83H significantly increased the proliferation of SKOV3 cells, but the proliferative effect was attenuated by co-knockdown of PD-L1 or β-catenin (Fig. 6B and 6C). To evaluate *in vivo* tumor growth and peritumoral immune cell infiltration according to FAM83H expression, we evaluated an *in vivo* xenograft tumor model using BALB/c nude mice and C57BL/6J mice (Fig. 7A). In nude mice, tumor growth was significantly decreased with knockdown of FAM83H and significantly increased with overexpression of FAM83H (Fig. 7B). Thereafter, tumor cubes derived from the BALB/c nude mice were implanted in the backs of C57BL/6J mice that maintain host immunity (Fig. 7A). Similar to the *in vitro* data shown in Figure 4, the overexpression of FAM83H was related to increased expression of PD-L1 and β-catenin, and the knockdown of FAM83H was related to the loss of PD-L1 and β-catenin expression, as shown by immunofluorescence staining of tumor tissue from C57BL/6J mice (Fig. 7C). Furthermore, overexpression of FAM83H was associated with more infiltration of FOXP3-positive regulatory T cells and PD1-positive lymphoid cells and decreased infiltration of CD8-positive cytotoxic T cells (Fig. 7D). In contrast, knockdown of FAM83H was associated with decreased infiltration of FOXP3-positive regulatory T cells and PD1-positive lymphoid cells and increased infiltration of CD8-positive cytotoxic T cells (Fig. 7D). These results

suggest that, in addition to interaction of FAM83H with PD-L1 and β-catenin, FAM83H is involved in the regulation of antitumor immune cell infiltration.

Discussion

In our results, there was a significant association between the immunohistochemical expression of FAM83H, PD-L1, and β-catenin and their individual, and combined expression patterns were significantly associated with the survival of ovarian carcinoma patients. In particular, FAM83H positivity and β-catenin positivity were independent indicators of shorter OS and RFS in ovarian carcinoma patients. Similarly, higher expression of FAM83H was significantly associated with shorter survival in patients with cancers of the breast [15], colorectum [29], stomach [8], liver [6], kidney [30], pancreas [16], and osteosarcoma [7]. The prognostic impact of β-catenin expression has also been reported in gastric cancer [8] and osteosarcoma patients [7]. Consistently, a positive association between FAM83H and active β-catenin expression in human tissue samples has been reported in human gastric carcinoma [8] and osteosarcomas [7]. With respect to the immunohistochemical expression of PD-L1, there are conflicting reports on the prognosis of cancer patients. Higher expression of PD-L1 predicts shorter survival in patients with soft-tissue sarcomas [31], pancreatic cancer [32], and gastric carcinomas [33]. In contrast, higher expression of PD-L1 was associated with a significantly favorable prognosis in patients with high-grade serous carcinoma of the ovary [34, 35]. However, despite controversial reports, PD-L1 positivity is important in the selection of patients for PD-L1/PD1-targeted immune checkpoint inhibitor therapy [12].

Furthermore, the combined expression patterns of FAM83H, PD-L1, and β-catenin are also useful for predicting the survival of ovarian carcinoma patients. Furthermore, the combined expression patterns of FAM83H, PD-L1, and β-catenin were also highly predictive of the survival of ovarian carcinoma patients. Patients having tumors with negative results for three markers had a 73% 10-year OS rate and a 59% 10-year RFS rate; in contrast, patients having tumors with positive results for three markers had only a 4% 10-year OS rate and a 0% 10-year RFS rate. These results suggest that the interconnected roles of FAM83H, PD-L1, and β-catenin might be involved in ovarian cancer progression. Considering the 51% 5-year relative survival rate of patients with ovarian cancer between 2013 and 2019 [18], the 76% 5-year OS rate of patients with low combined scores (scores of 0 and 1) and the 35% 5-year OS rate of patients with high scores (scores of 2 and 3) of ovarian carcinoma suggest that this combined score might be helpful for predicting the survival of patients.

In addition, when we performed survival analysis according to the histologic subtypes, although there was a limitation in the number of cases, FAM83H positivity was an independent indicator of OS (HR; 2.328, 95% CI; 1.276-4.244, $P = 0.006$) and RFS (HR; 1.708, 95% CI; 1.008-2.895, $P = 0.047$) in high-grade serous carcinoma patients in multivariate analysis. Positivity for β-catenin was also an independent prognostic indicator of OS (HR; 2.206, 95% CI; 1.196-4.071, $P = 0.001$). The coexpression patterns of FAM83H, PD-L1, and β-catenin also predicted OS (Model 1; overall $P = 0.010$, Model 2; $P = 0.002$) in multivariate analysis of high-grade serous carcinomas. Therefore, as high-grade serous carcinoma is considered the most common and aggressive ovarian cancer type, these results suggest that the expression of FAM83H, PD-L1, and β-catenin might be used as prognostic

indicators of ovarian carcinomas, especially high-grade serous carcinomas.

In this study, one of the interesting findings is that FAM83H, PD-L1, and β-catenin are involved in the stabilization of each other by prevention of proteasomal degradation. First, consistent with the positive correlation between FAM83H, PD-L1, and β-catenin in tissue samples, molecular docking analysis and immunoprecipitation data revealed that FAM83H, PD-L1, and β-catenin directly bind and form a complex. In addition, knockdown of either FAM83H, PD-L1, or β-catenin accelerated the degradation of the other two proteins. Moreover, the pro-proliferative effects of FAM83H in ovarian cancer cells were influenced by the co-knockdown of PD-L1 or β-catenin. The increased proliferation of cells overexpressing FAM83H was attenuated by the knockdown of PD-L1 or β-catenin. FAM83H knockdown-mediated suppression of cellular proliferation was accentuated by knockdown of PD-L1 or β-catenin. The roles of FAM83H in the proliferation and invasion/metastatic potential of cancer cells are associated with interactions with MYC [6], SCRIB [8], the Wnt/β-catenin pathway [7, 8], KRAS [16], and the EMT pathway [8] in various human cancers. The impact of the expression of PD-L1 and β-catenin on cellular proliferation has also been reported in various human cancers [14, 20]. Therefore, our results suggest that FAM83H, PD-L1, and β-catenin are cooperatively involved in the progression of ovarian cancer. However, there are more complex molecular relationships associated with the FAM83H/PD-L1/β-catenin relationship in cancer progression. The expression and stabilization of FAM83H, PD-L1, and β-catenin are also affected by various molecules. FAM83H is transcriptionally controlled by MYC in liver cancer [6] and cooperatively affects cancer progression *via* direct binding to SCRIB in gastric cancer [8]. The expression and

stabilization of PD-L1 are affected by various mechanisms, including MYC [36], stabilization by PAK4 [25], ubiquitination by β-TrCP [17], and are negatively regulated by estrogen receptors in ovarian cancer [37]. Fibronectin type III domain-containing 3B (FNDC3B) inhibited the proteasomal degradation of FAM83H by directly interacting with it and stimulating the EMT pathway in gastric cancer [38]. In colorectal cancer, TRIM29 also stabilizes FAM83H by inhibiting its ubiquitination and promotes its metastatic activity through the redistribution of cellular keratins [39]. The expression of β-catenin is regulated by various components of the degradation complex [14], and FAM83H and SCRIB are also involved in its posttranslational stabilization by interrupting the interaction between β-catenin and β-TrCP [8]. Therefore, although we focused on the relationships among FAM83H, PD-L1, and β-catenin, more molecules, including β-TrCP, which is a mediator between FAM83H, PD-L1, and β-catenin, might be involved in a complex manner in the regulation of homeostasis and oncogenesis in human cancers, and further study is needed to understand these complex mechanisms.

In this study, the molecular relationship between FAM83H and PD-L1 suggest that FAM83H might be involved in anticancer host immunity. In our *in vivo* tumor model, overexpression of FAM83H was associated with increased infiltration of PD1-positive cells and FOXP3-positive regulatory T cells, and decreased infiltration of CD8-positive cytotoxic T cells, and *vice versa* with knockdown of FAM83H. Similarly, a positive association between FAM83H expression and infiltration of PD1-positive lymphocytes in breast cancer has been reported [15]. Positive nuclear expression of FAM83H was significantly associated with more PD1-positive cell infiltration [15]. Consistently, higher expression of FAM83H

was associated with decreased intratumoral infiltration of CD8-positive T cells in pancreatic cancer [16] and gastric cancer [40]. Moreover, β-catenin is involved in the immune evasion of cancer cells through the regulation of PD-L1 expression [13], and our results also showed that β-catenin is involved in the stabilization of PD-L1 and FAM83H. Recently, the use of immune checkpoint inhibitors targeting the PD1/PD-L1 interaction has proven effective in the treatment of cancer patients, especially in advanced cancers [9]. However, despite successful effects in some populations of cancer patients, it is not effective, or some populations of patients have acquired resistance to immune checkpoint inhibitors [9, 10]. Therefore, more understanding of the mechanism of anticancer immunity between cancer cells and the environment is needed [10]. As a strategy to overcome the limitations of immune checkpoint inhibitors, combinations with other chemotherapeutic agents and complex immune modulators are under evaluation in the clinical field [9, 10]. In addition, our clinical data revealed that higher expression of FAM83H, PD-L1, and β-catenin were significantly associated with increased platinum-resistance in ovarian carcinomas. This chemoresistance might be related to the roles of Wnt/β-catenin and the FAM83H-mediated EMT pathway in chemoresistance. In this context, in addition to the relationships between FAM83H, PD-L1, and β-catenin to stabilize each other, our results suggest that they are cooperatively involved in cellular proliferation and the modulation of the anticancer host immune environment.

Conclusions

In conclusion, this study showed that the individual and combined expression patterns of FAM83H, PD-L1, and β-catenin might be used as prognostic indicators of ovarian carcinoma. In addition, we showed that FAM83H, PD-L1, and β-catenin form a complex that stabilizes each other and stimulates the proliferation of ovarian cancer cells. Furthermore, FAM83H expression was associated with the peritumoral antitumor immune environment. Therefore, strategies that block or interrupt the association between FAM83H, PD-L1, and β-catenin might be effective in both the inhibition of the cancer progression pathway and the modulation of the anticancer immune environment.

Abbreviations

EMT (epithelial-to-mesenchymal transition), GEO (Gene Expression Omnibus), HR (hazard ratio), MTT (3-(4,5-dimethylthiazol-2-yl)-2,5-diphenyltetrazolium bromide), OS (overall survival), RFS (relapse-free survival), TMA (tissue microarray), 95% CI (95% confidence interval), 5y-OS (OS rate at 5 years), 10y-OS (OS rate at 10 years), 5y-RFS (RFS rate at 5 years), 10y-RFS (RFS rate at 10 years).

Ethics approval and consent to participate

This study was approved by the institutional review board of Jeonbuk National University Hospital (IRB number, CUH 2025-05-004; approval date, May 14, 2025) and was performed according to the Declaration of Helsinki. Written informed consent was waived during approval of the IRB based on the retrospective and anonymous nature of the study. All animal experiments were performed with the Institutional Animal Care and Use Committee of

Jeonbuk National University (IRB number, JBNU NON2025-073-001; approval date, June 12, 2025).

Consent for publication

Not applicable

Availability of data and materials

The datasets used in the current study are available from the corresponding author upon reasonable request.

Competing interests

The authors declare that they have no competing interests.

Funding

This work was supported by a grant of the Korea Health Technology R&D Project through the Korea Health Industry Development Institute (KHIDI), funded by the Ministry of Health & Welfare, Republic of Korea (grant number: HR22C1832).

Authors' contributions

JZ, KMK, HSK, WKC, ARA, HSP, SHP, DHC, YJM and KYJ participated in the study design. JZ, KMK, HSK, WKC, ARA, HSP, SHP, DHC, YJM and KYJ performed the experiments. JZ, KMK, HSK, WKC, HSP, DHC, YJM and KYJ were involved in data

collection and data interpretation. JZ, KMK, HSK, WKC, ARA, YJM and KYJ participated in the statistical analyses. JZ, KMK, HSK, WKC, ARA, HSP, SHP, DHC, YJM and KYJ wrote the manuscript. All authors read and approved the final manuscript.

Acknowledgments

We thank DB Leveson-Gower, who provided medical writing services.

References

1. Hart PS, Becerik S, Cogulu D, Emingil G, Ozdemir-Ozenen D, Han ST, Sulim a PP, Firatli E, Hart TC. Novel FAM83H mutations in Turkish families with a utosomal dominant hypocalcified amelogenesis imperfecta. Clin Genet. 2009;75 (4):401-4.
2. Kim JW, Lee SK, Lee ZH, Park JC, Lee KE, Lee MH, Park JT, Seo BM, Hu JC, Simmer JP. FAM83H mutations in families with autosomal-dominant hypo calcified amelogenesis imperfecta. Am J Hum Genet. 2008;82(2):489-94.
3. Kuga T, Kume H, Kawasaki N, Sato M, Adachi J, Shiromizu T, Hoshino I, N ishimori T, Matsubara H, Tomonaga T. A novel mechanism of keratin cytoskel eton organization through casein kinase Iα and FAM83H in colorectal cancer. J Cell Sci. 2013;126(20):4721-31.
4. Snijders AM, Lee SY, Hang B, Hao W, Bissell MJ, Mao JH. FAM83 family o ncogenes are broadly involved in human cancers: an integrative multi-omics ap proach. Mol Oncol. 2017;11(2):167-79.
5. Lin S, Du J, Hao J, Luo X, Wu H, Zhang H, Zhao X, Xu L, Wang B. Identi fication of Prognostic Biomarkers Among FAM83 Family Genes in Human Ov arian Cancer Through Bioinformatic Analysis and Experimental Verification. Ca ncer Manag Res. 2021;13:8611-27.
6. Kim KM, Park SH, Bae JS, Noh SJ, Tao GZ, Kim JR, Kwon KS, Park HS, Park BH, Lee H *et al*. FAM83H is involved in the progression of hepatocellul ar carcinoma and is regulated by MYC. Sci Rep. 2017;7(1):3274.
7. Kim KM, Hussein UK, Park SH, Kang MA, Moon YJ, Zhang Z, Song Y, Par k HS, Bae JS, Park BH *et al*. FAM83H is involved in stabilization of beta-cat enin and progression of osteosarcomas. J Exp Clin Cancer Res. 2019;38(1):267.
8. Hussein UK, Ha SH, Ahmed AG, Kim KM, Park SH, Kim CY, Kwon KS, Z hang Z, Lee SA, Park HS *et al*. FAM83H and SCRIB stabilize beta-catenin an d stimulate progression of gastric carcinoma. Aging (Albany NY). 2020;12(12): 11812-34.

9. Wang Y, Wang M, Wu HX, Xu RH. Advancing to the era of cancer immunotherapy. Cancer Commun (Lond). 2021;41(9):803-29.
10. Chen X, Feng L, Huang Y, Wu Y, Xie N. Mechanisms and Strategies to Overcome PD-1/PD-L1 Blockade Resistance in Triple-Negative Breast Cancer. Cancers (Basel). 2022;15(1).
11. Ding P, Ma Z, Fan Y, Feng Y, Shao C, Pan M, Zhang Y, Huang D, Han J, Hu Y *et al*. Emerging role of ubiquitination/deubiquitination modification of PD-1/PD-L1 in cancer immunotherapy. Genes Dis. 2023;10(3):848-63.
12. Akhtar M, Rashid S, Al-Bozom IA. PD-L1 immunostaining: what pathologists need to know. Diagn Pathol. 2021;16(1):94.
13. Martin-Orozco E, Sanchez-Fernandez A, Ortiz-Parra I, Ayala-San Nicolas M. WNT Signaling in Tumors: The Way to Evade Drugs and Immunity. Front Immunol. 2019;10:2854.
14. Song P, Gao Z, Bao Y, Chen L, Huang Y, Liu Y, Dong Q, Wei X. Wnt/beta-catenin signaling pathway in carcinogenesis and cancer therapy. J Hematol Oncol. 2024;17(1):46.
15. Choi JE, Ahn AR, Zhang J, Kim KM, Park HS, Lee H, Chung MJ, Moon WS, Jang KY. FAM83H Expression Is Associated with Tumor-Infiltrating PD1-Positive Lymphocytes and Predicts the Survival of Breast Carcinoma Patients. Diagnostics (Basel). 2023;13(18).
16. Zhuang H, Zhang C, Hou B. FAM83H overexpression predicts worse prognosis and correlates with less CD8(+) T cells infiltration and Ras-PI3K-Akt-mTOR signaling pathway in pancreatic cancer. Clin Transl Oncol. 2020;22(12):2244-52.
17. Zhang F, Jiang R, Sun S, Wu C, Yu Q, Awadasseid A, Wang J, Zhang W. Recent advances and mechanisms of action of PD-L1 degraders as potential therapeutic agents. Eur J Med Chem. 2024;268:116267.
18. Siegel RL, Giaquinto AN, Jemal A. Cancer statistics, 2024. CA Cancer J Clin. 2024;74(1):12-49.
19. Chen K, Wang J, Yang M, Deng S, Sun L. Immunotherapy in Recurrent Ovari

an Cancer. Biomedicines. 2025;13(1).

20. Chen J, Jiang CC, Jin L, Zhang XD. Regulation of PD-L1: a novel role of pro-survival signalling in cancer. Ann Oncol. 2016;27(3):409-16.

21. Board WCoTE. Female genital tumours, 5th edn. Lyon (France): International Agency for Research on Cancer; 2020.

22. Amin MB, American Joint Committee on Cancer., American Cancer Society. AJCC cancer staging manual, 8th edn. Chicago IL: American Joint Committee on Cancer, Springer; 2017.

23. Therasse P, Arbuck SG, Eisenhauer EA, Wanders J, Kaplan RS, Rubinstein L, Verweij J, Van Glabbeke M, van Oosterom AT, Christian MC *et al*. New guidelines to evaluate the response to treatment in solid tumors. European Organization for Research and Treatment of Cancer, National Cancer Institute of the United States, National Cancer Institute of Canada. J Natl Cancer Inst. 2000;92(3):205-16.

24. Allred D, Harvey JM, Berardo M, Clark GM. Prognostic and predictive factors in breast cancer by immunohistochemical analysis. Mod Pathol. 1998;11(2):155-68.

25. Zhang J, Song Y, Ahn AR, Park HS, Park SH, Moon YJ, Kim KM, Jang KY. PAK4 Is Involved in the Stabilization of PD-L1 and the Resistance to Doxorubicin in Osteosarcoma and Predicts the Survival of Diagnosed Patients. Cells. 2024;13(17).

26. Ahmad S, Jose da Costa Gonzales L, Bowler-Barnett EH, Rice DL, Kim M, Wijerathne S, Luciani A, Kandasaamy S, Luo J, Watkins X *et al*. The UniProt website API: facilitating programmatic access to protein knowledge. Nucleic Acids Res. 2025;53(W1):W547-W53.

27. Yan Y, Tao H, He J, Huang SY. The HDOCK server for integrated protein-protein docking. Nat Protoc. 2020;15(5):1829-52.

28. DeLong ER, DeLong DM, Clarke-Pearson DL. Comparing the areas under two or more correlated receiver operating characteristic curves: a nonparametric appr

oach. Biometrics. 1988;44(3):837-45.

29. Jeong TY, Lee HI, Park MS, Seo MY, Jang KY. Individual and Co-Expression Patterns of FAM83H and SCRIB at Diagnosis Are Associated with the Surviva l of Colorectal Carcinoma Patients. Diagnostics (Basel). 2022;12(7).

30. Kim KM, Hussein UK, Bae JS, Park SH, Kwon KS, Ha SH, Park HS, Lee H, Chung MJ, Moon WS *et al*. The Expression Patterns of FAM83H and PAN X2 Are Associated With Shorter Survival of Clear Cell Renal Cell Carcinoma Patients. Front Oncol. 2019;9:14.

31. Kim JR, Moon YJ, Kwon KS, Bae JS, Wagle S, Kim KM, Park HS, Lee H, Moon WS, Chung MJ *et al*. Tumor infiltrating PD1-positive lymphocytes and t he expression of PD-L1 predict poor prognosis of soft tissue sarcomas. PLoS One. 2013;8(12):e82870.

32. Nomi T, Sho M, Akahori T, Hamada K, Kubo A, Kanehiro H, Nakamura S, E nomoto K, Yagita H, Azuma M *et al*. Clinical significance and therapeutic pot ential of the programmed death-1 ligand/programmed death-1 pathway in huma n pancreatic cancer. Clin Cancer Res. 2007;13(7):2151-7.

33. Wu C, Zhu Y, Jiang J, Zhao J, Zhang XG, Xu N. Immunohistochemical locali zation of programmed death-1 ligand-1 (PD-L1) in gastric carcinoma and its cli nical significance. Acta Histochem. 2006;108(1):19-24.

34. Darb-Esfahani S, Kunze CA, Kulbe H, Sehouli J, Wienert S, Lindner J, Budcz ies J, Bockmayr M, Dietel M, Denkert C *et al*. Prognostic impact of program med cell death-1 (PD-1) and PD-ligand 1 (PD-L1) expression in cancer cells a nd tumor-infiltrating lymphocytes in ovarian high grade serous carcinoma. Onco target. 2016;7(2):1486-99.

35. Webb JR, Milne K, Kroeger DR, Nelson BH. PD-L1 expression is associated with tumor-infiltrating T cells and favorable prognosis in high-grade serous ova rian cancer. Gynecol Oncol. 2016;141(2):293-302.

36. Casey SC, Tong L, Li Y, Do R, Walz S, Fitzgerald KN, Gouw AM, Baylot V, Gutgemann I, Eilers M *et al*. MYC regulates the antitumor immune response

through CD47 and PD-L1. Science. 2016;352(6282):227-31.

37. Shuai C, Yang X, Pan H, Han W. Estrogen Receptor Downregulates Expressio n of PD-1/PD-L1 and Infiltration of CD8(+) T Cells by Inhibiting IL-17 Signal ing Transduction in Breast Cancer. Front Oncol. 2020;10:582863.

38. Zhang Y, Ran L, Liu Y, Li W, Ran A, Li H, Huang B, Ren J, Ning H, Ma Q *et al*. FNDC3B promotes gastric cancer metastasis via interacting with FAM 83H and preventing its proteasomal degradation. Cell Mol Biol Lett. 2025;30 (1):65.

39. Fu Y, Huang R, Qin G, Huang S, Li J, Zhan W, Bai F, Xie X, Ling J, Cai Y *et al*. TRIM29 promotes liver metastasis via enhancing hepatic colonization by stabilizing FAM83H to regulate keratin network in colorectal cancer. Cell Si gnal. 2025;134:111871.

40. Zhang T, Lai S, Cai Y, Huang Z, Li Y, Chen S, Zhang Z, Ye Z, Lai X, Zhai E *et al*. Comprehensive Analysis and Identification of Prognostic Biomarkers and Therapeutic Targets Among FAM83 Family Members for Gastric Cancer. F ront Cell Dev Biol. 2021;9:719613.

Figure legends

Fig. 1 Immunohistochemical staining and survival analysis of human ovarian carcinomas. **A** Negative and positive expression of immunohistochemical staining for FAM83H, PD-L1, and β-catenin in serous, mucinous, and endometroid carcinoma of the ovary. Original magnification, ×400. **B** Receiver operating curve statistical analysis to determine cutoff points of immunohistochemical staining scores for FAM83H (red arrow), PD-L1 (blue arrow), and β-catenin (green arrow). The points with the highest area under the curve were selected as cutoff points to predict the death of patients from ovarian carcinomas. **c** Kaplan-Meier survival analysis for overall survival and relapse-free survival according to the positivity for FAM83H, PD-L1, and β-catenin immunostaining.

Fig. 2 Kaplan-Meier survival analysis in 77 high-grade serous carcinomas and 34 mucinous carcinomas. **A** Overall and relapse-free survival curves in high-grade serous carcinomas. **B** Overall and Relapse-free survival curves in mucinous carcinomas.

Fig. 3 Kaplan-Meier survival analysis according to combined expression patterns of FAM83H, PD-L1, and β-catenin. **A** Survival curves for overall survival and relapse-free survival according to the number of positive markers from FAM83H, PD-L1, and β-catenin in 150 ovarian carcinomas. The score was zero (negative for three markers), one (positive for one of three markers), two (positive for two of three markers), or three (positive for three markers). **B** Kaplan-Meier survival curves according to two subgroups (scores 0 and 1 *versus*

scores 2 and 3) of combined expression patterns of FAM83H, PD-L1, and β-catenin in 150 ovarian carcinomas. **C-E** Survival curves according to two subgroups of combined expression patterns in 21 low-grade serous carcinomas (**C**), 77 high-grade serous carcinomas (**D**), and 34 mucinous carcinomas (**E**).

Fig. 4 The expression patterns of FAM83H, PD-L1, and β-catenin in ovarian carcinomas. **A** Expression of the FAM83H gene in normal ovarian tissue and ovarian carcinoma tissue from the GEPIA database. **B** Differentially expressed genes (DEGs) identified by searching the Gene Expression Omnibus database. DEGs were identified using a threshold of $\log_2$-fold change greater than 1 and $P < 0.05$. Sixteen overlapping genes, including FAM83H, were found across the four datasets. **C** Predicted protein–protein interactions *via* molecular docking analysis. The interactions were analyzed using AutoDock and visualized *via* PyMol software. The protein–protein interactions were analyzed *via* HDOCK SERVICE. There is strong potential for real binding between FAM83H, PD-L1, and β-catenin: between FAM83H (green) and β-catenin (blue); between FAM83H (green) and PD-L1 (red); between PD-L1 (red) and β-catenin (blue); and between FAM83H (green), PD-L1 (red), and β-catenin (blue). **D-F** Western blot and quantitative reverse-transcription polymerase chain reaction results after knockdown or overexpression of FAM83H (**D**), knockdown of PD-L1 (**E**), and knockdown of β-catenin (**F**). **G** SKOV3 and OVCAR3 ovarian cancer cells were transfected with empty vectors (EVs; empty vector and control vector for shRNA), wild-type FAM83H, or shRNA for FAM83H and immunofluorescence staining performed for FAM83H (red), β-catenin (green), and PD-L1 (yellow) and counterstained with 4′,6-diamidino-2-phenylindole

(DAPI, blue). **H** SKOV3 and OVCAR3 ovarian cancer cells were transfected with control vectors for shRNA, shRNA for β-catenin, or shRNA for PD-L1, and performed immunofluorescence staining for β-catenin (red), FAM83H (yellow), and PD-L1 (green), and counterstained with 4′,6-diamidino-2-phenylindole (DAPI, blue). Images were taken with an APX100 microscope. The scale bar is 10 μm. ** $P < 0.001$; *ns*, not significant; EV, empty vector; FAM83H-OE, vector for wild-type FAM83H; shControl, control vector for shRNA; shFAM83H, vector for shRNA for FAM83H; shPD-L1, vector for shRNA for PD-L1; shβ-catenin, vector for shRNA for β-catenin.

Fig. 5 FAM83H, PD-L1, and β-catenin directly bind and stabilize each other. **A** SKOV3 and OVCAR3 cells were immunoprecipitated with FAM83H, PD-L1, or β-catenin and immunoblotted with FAM83H, PD-L1, and β-catenin. **B** SKOV3 cells were transfected with the control vector for shRNA or shRNA for FAM83H and treated with 30 μM cycloheximide or 30 μM MG132 for 0.5 to 2.0 hours. Thereafter, the protein lysates were immunoblotted with antibodies against PD-L1, β-catenin, and GAPDH. **C** Total protein lysate from SKOV3 cells transfected with empty vector for shRNA or shRNA for FAM83H and treated with 30 μM MG132 for two hours was immunoprecipitated with PD-L1 or β-catenin and immunoblotted with anti-ubiquitin. Input protein lysates were immunoblotted with anti-FAM83H, anti-PD-L1, anti-β-catenin, and anti-actin antibodies. **D** Total protein lysate from SKOV3 cells transfected with empty vector for shRNA or shRNA for PD-L1 and treated with 30 μM MG132 for two hours was immunoprecipitated with FAM83H or β-catenin and immunoblotted with anti-ubiquitin. Input protein lysates were immunoblotted with anti-

FAM83H, anti-PD-L1, anti-β-catenin, and anti-actin antibodies. **E** Total protein lysate from SKOV3 cells transfected with empty vector for shRNA or shRNA for β-catenin and treated with 30 μM MG132 for two hours was immunoprecipitated with FAM83H and PD-L1 and immunoblotted with anti-ubiquitin. Input protein lysates were immunoblotted with anti-FAM83H, anti-PD-L1, anti-β-catenin, and anti-actin antibodies. CHX, cycloheximide; IP, immunoprecipitation; IB, immunoblotting; FAM83H-OE, vector for wild-type FAM83H; shControl, control vector for shRNA; shFAM83H, vector for shRNA for FAM83H; shPD-L1, vector for shRNA for PD-L1; shβ-catenin, vector for shRNA for β-catenin.

Fig. 6 FAM83H, PD-L1, and β-catenin are cooperatively involved in the proliferation of ovarian cancer cells. **A** SKOV3 cell line, in which FAM83H was knocked down or overexpressed, was cotransfected with a control vector for shRNA, shRNA for PD-L1, or shRNA for β-catenin, followed by western blotting for FAM83H, PD-L1, β-catenin, and actin. **B** MTT proliferation assays were performed by cotransfecting 2×10^3 SKOV3 cells with the indicated plasmids for 24, 48, or 72 hours. **C** Colony-forming assays were performed after 2×10^3 SKOV3 cells were cotransfected with the indicated plasmids for seven days. * $P < 0.05$; ** $P < 0.001$; ns, not significant; EVs, empty vectors for empty vector for wild-type FAM83H and control vector for shRNA; FAM83H-OE, vector for wild-type FAM83H; shControl, control vector for shRNA; shFAM83H, vector for shRNA for FAM83H; shPD-L1, vector for shRNA for PD-L1; shβ-catenin, vector for shRNA for β-catenin.

Fig. 7 *In vivo* evaluation of immune cell infiltration according to the expression of FAM83H.

A SKOV3 ovarian cancer cells (2.5×10^6) transfected with empty vectors (EVs), a vector for shRNA for FAM83H, or a vector for wild-type FAM83H were implanted subcutaneously into the backs of BALB/c nude mice and grown for six weeks. Donor tumor blocks $2 \times 2 \times 2$ mm³ in size from the resected tumors of BALB/c nude mice were subcutaneously implanted in the backs of C57BL/6J mice and evaluated histologically four days after implantation. The figure was created with BioRender.com (https://www.biorender.com, accessed on 1 August 2025). **B** *In vivo* growth of OVCA3 cells transfected with empty vectors (EVs), a vector for shRNA for FAM83H, or a vector for wild-type FAM83H in BALB/c nude mice. **C** Four days after the implantation of tumor blocks in C57BL/6J mice, the tumors and surrounding tissue were resected and evaluated with H&E staining and immunofluorescence staining for FAM83H (red) and PD-L1 (green) or FAM83H (red) and β-catenin (green). Scale bars, 20 μm. **D** Immunofluorescence staining for FOXP3, PD1, CD4, and CD8 in resected tissue containing tumors from C57BL/6J mice. The number of positively stained cells was counted in three high-power fields in each case, and the sum of the numbers was used for evaluation. The area of one high-power field image was 0.00367 mm^2. Therefore, 0.01101 mm² was evaluated in each case. * $P < 0.05$ *versus* EVs; ** $P < 0.001$ *versus* EVs; *ns*, not significant *versus* EVs; EVs, empty vectors; FAM83H-OE, vector for wild-type FAM83H; shFAM83H, vector for shRNA for FAM83H.

Tables

Table 1 Association between clinicopathologic variables and the expression of FAM83H, PD-L1, and β-catenin

Characteristics		No.	FAM83H		PD-L1		β-catenin	
			Positive	*P*	Positive	*P*	Positive	*P*
Age, y	< 60	105	44 (42%)	0.042	47 (45%)	0.335	52 (50%)	0.356
	≥ 60	45	27 (60%)		24 (53%)		26 (58%)	
CA125	Normal	30	6 (20%)	0.001	9 (30%)	0.027	12 (40%)	0.093
	Elevated	110	58 (53%)		58 (53%)		63 (57%)	
TNM stage	I & II	67	19 (28%)	< 0.001	22 (33%)	0.001	29 (43%)	0.074
	III & IV	81	51 (63%)		48 (59%)		47 (58%)	
Tumor size, cm	≤ 10	90	46 (51%)	0.256	46 (51%)	0.256	55 (61%)	0.006
	> 10	60	25 (42%)		25 (42%)		23 (38%)	
LN metastasis	Absence	125	55 (44%)	0.096	59 (47%)	0.801	64 (51%)	0.790
	Presence	24	15 (63%)		12 (50%)		13 (54%)	
Ascites	Absence	103	47 (46%)	0.536	43 (42%)	0.043	50 (49%)	0.210
	Presence	47	24 (51%)		28 (60%)		28 (60%)	
Bilaterality	Unilateral	78	31 (40%)	0.064	29 (37%)	0.007	39 (50%)	0.668
	Bilateral	71	39 (55%)		42 (59%)		38 (54%)	
Histologic type	Low-grade serous	21	10 (48%)	0.001	4 (19%)	< 0001	9 (43%)	0.003
	High-grade serous	77	49 (64%)		51 (66%)		50 (65%)	
	Mucinous	34	8 (24%)		12 (35%)		12 (35%)	
	Endometrioid	11	2 (18%)		3 (27%)		7 (64%)	
	Clear cell	5	1 (20%)		1 (20%)		0 (0%)	
	Malignant Brenner	2	1 (50%)		0 (0%)		0 (0%)	
Platinum-resistance	Absence	70	27 (39%)	0.016	29 (41%)	0.006	31 (44%)	0.014
	Presence	48	29 (60%)		32 (67%)		32 (67%)	
β-catenin	Negative	72	27 (38%)	0.020	24 (33%)	< 0.001		
	Positive	78	44 (56%)		47 (60%)			
PD-L1	Negative	79	22 (28%)	< 0.001				
	Positive	71	49 (69%)					

Abbreviations: TNM, tumor, node, and metastasis; LN, lymph node.

Table 2 Univariate Cox regression analysis for overall survival and relapse-free survival in ovarian carcinomas

Characteristics	No.	OS		RFS	
		HR (95% CI)	*P*	HR (95% CI)	*P*
Age, y, ≥ 60 (*vs* < 60)	45/150	2.457 (1.580-3.821)	< 0.001	2.112 (1.399-3.188)	< 0.001
TNM stage, III & IV (*vs* I & II)	81/150	4.908 (2.849-8.455)	< 0.001	5.318 (3.251-8.697)	< 0.001
Tumor size, cm, > 10 (*vs* ≤ 10)	60/150	0.663 (0.416-1.058)	0.085	0.747 (0.491-1.135)	0.172
LN metastasis, presence (*vs* absence)	24/150	1.787 (1.054-3.029)	0.031	1.965 (1.215-3.179)	0.006
Ascites, presence (*vs* absence)	47/150	1.924 (1.236-2.996)	0.004	1.746 (1.161-2.624)	0.007
Bilaterality, bilateral (*vs* unilateral)	71/150	2.254 (1.428-3.557)	< 0.001	2.828 (1.847-4.329)	< 0.001
CA125, elevated (*vs* normal)	110/140	5.384 (2.169-13.364)	< 0.001	4.358 (2.103-9.034)	< 0.001
FAM83H, positive (*vs* negative)	71/150	3.184 (2.000-5.069)	< 0.001	2.769 (1.831-4.189)	< 0.001
PD-L1, positive (*vs* negative)	71/150	2.539 (1.609-4.007)	< 0.001	2.227 (1.480-3.350)	< 0.001
β-catenin, positive (*vs* negative)	78/150	2.568 (1.607-4.103)	< 0.001	1.931 (1.281-2.908)	0.002

Abbreviations: OS, overall survival; RFS, relapse-free survival; HR; hazard ratio, 95% CI; 95% confidence interval; TNM, tumor, node, and metastasis; LN, lymph node.

Table 3 Multivariate Cox regression analysis for overall survival and relapse-free survival in ovarian carcinomas

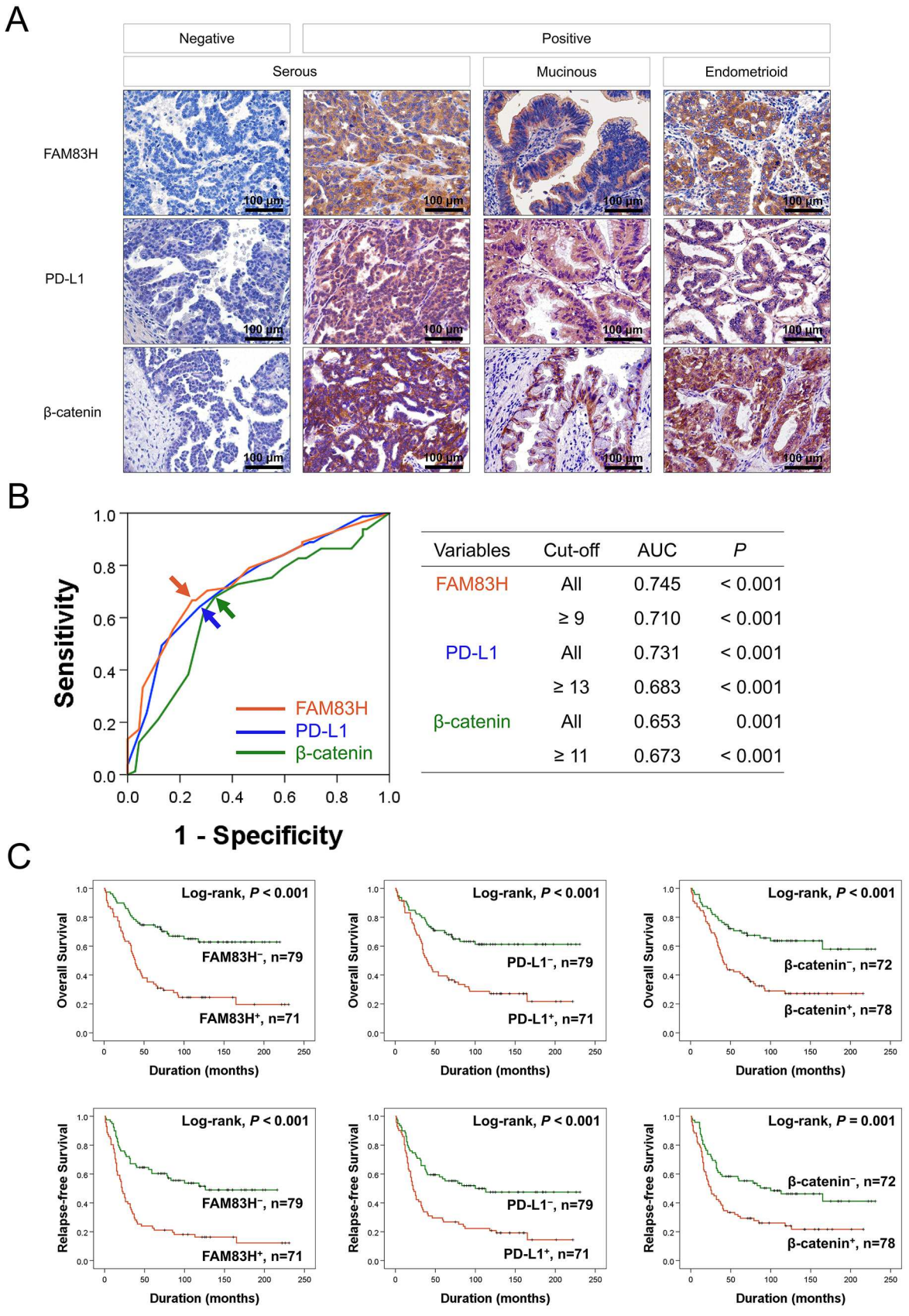
Characteristics	OS		RFS	
	HR (95% CI)	*P*	HR (95% CI)	*P*
Age, y, ≥ 60 (*vs* < 60)	1.975 (1.250-3.120)	0.004	1.661 (1.083-2.547)	0.020
TNM category, III & IV (*vs* I & II)	3.181 (1.785-5.669)	< 0.001	3.816 (2.266-6.424)	< 0.001
FAM83H, positive (*vs* negative)	1.924 (1.155-3.204)	0.012	1.823 (1.172-2.837)	0.008
β-catenin, positive (*vs* negative)	2.072 (1.281-3.352)	0.003	1.603 (1.047-2.454)	0.030

Abbreviations: OS, overall survival; RFS, relapse-free survival; HR; hazard ratio, 95% CI; 95% confidence interval; TNM, tumor, node, and metastasis. The multivariate analysis was performed with the factors significantly associated with OS and RFS: age, TNM stage, LN metastasis, ascites, bilaterality, and the expression of FAM83H, PD-L1, and β-catenin, but CA125 was not included because 10 patients did not measured their preoperative serum levels.

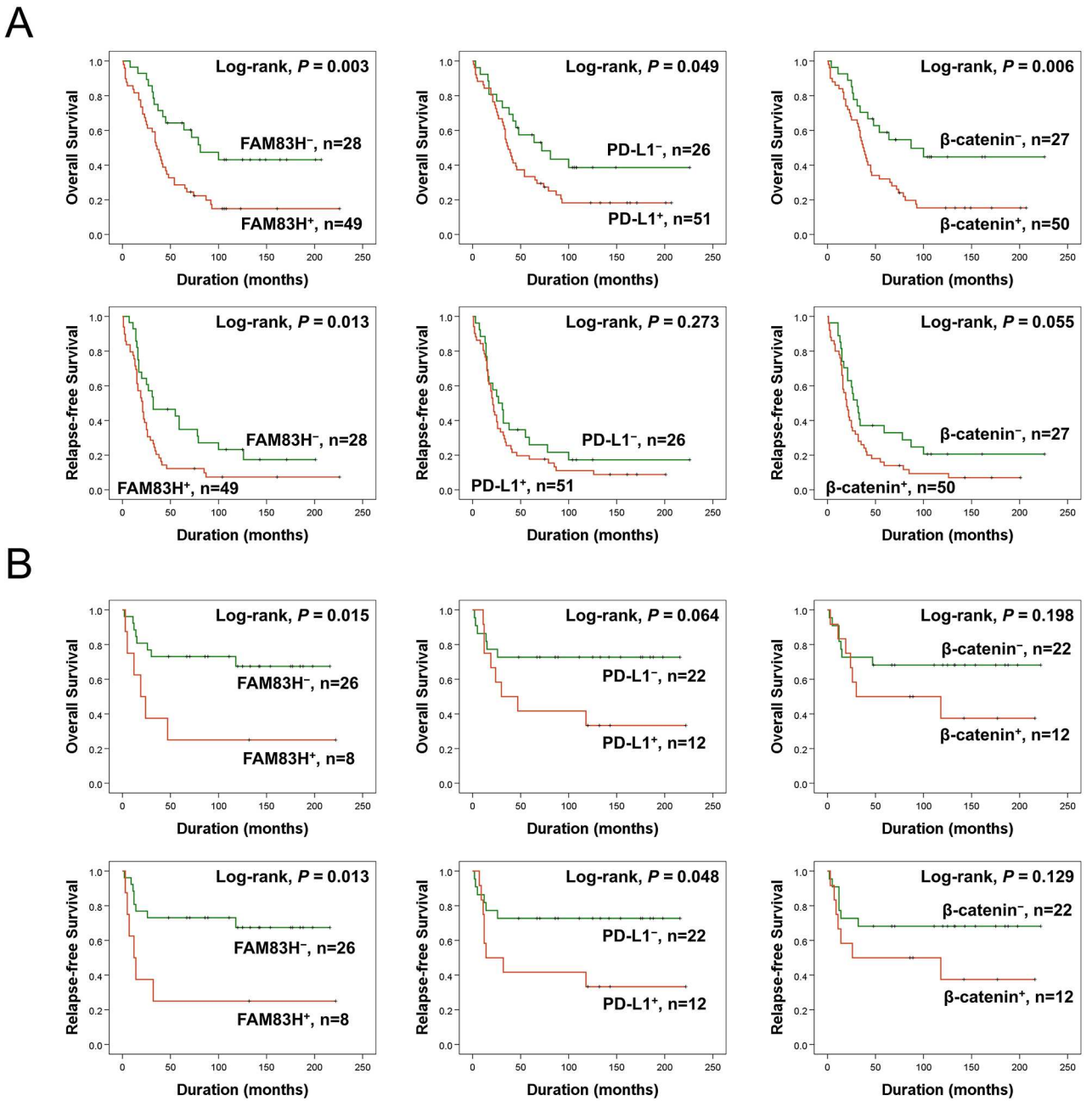
Table 4 Survival rate according to the combined expression patterns of FAM83H, PD-L1, and β-catenin.

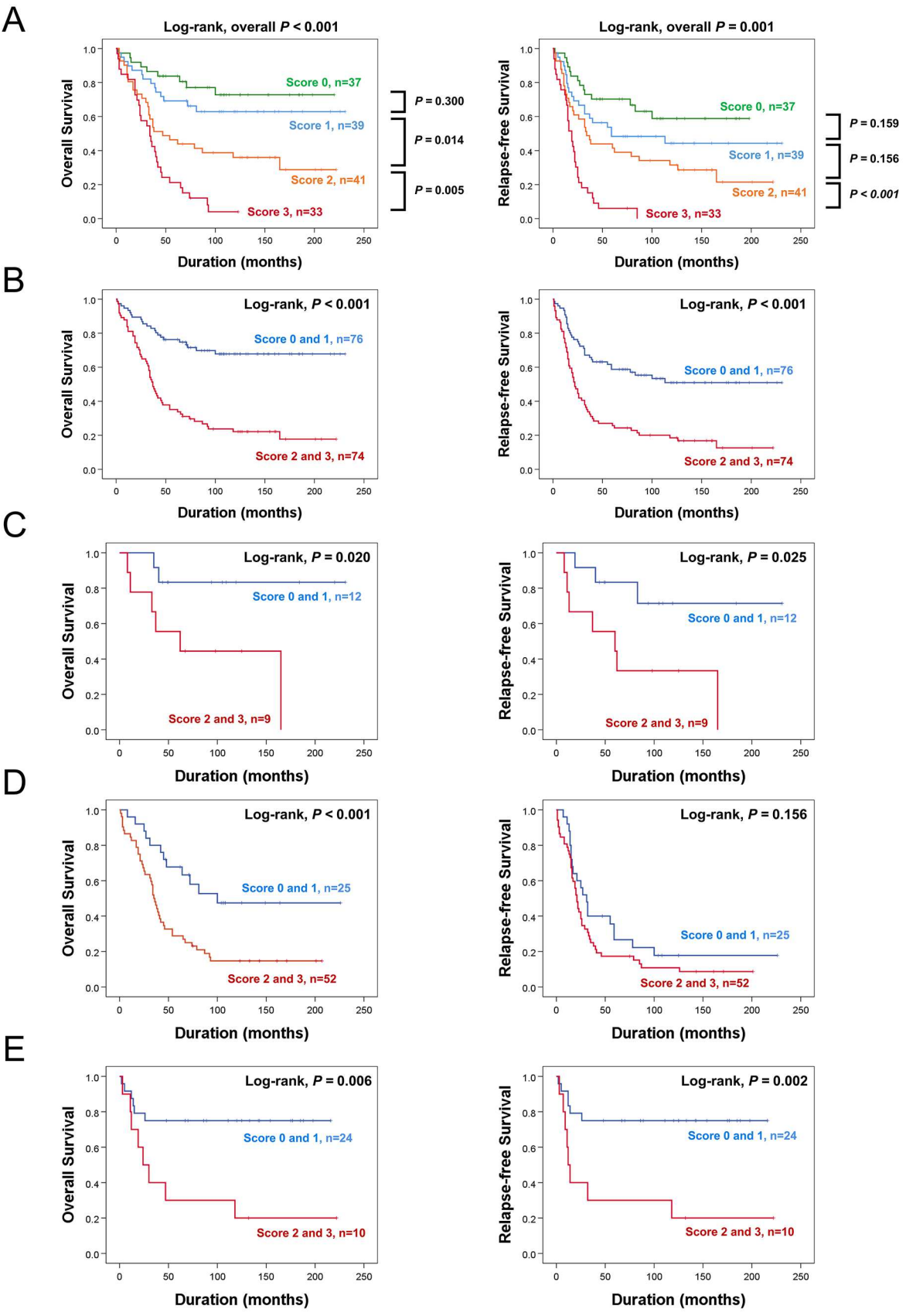
Combined expression pattern	No.	5y-OS (%)	10y-OS (%)	5y-RFS (%)	10y-RFS (%)
Combined expression Model 1					
score 0	37	84	73	70	59
score 1	39	69	63	48	44
score 2	41	46	36	41	32
score 3	33	21	4	6	0
Combined expression Model 2					
score 0 and 1	76	76	68	59	51
score 2 and 3	74	35	22	26	18

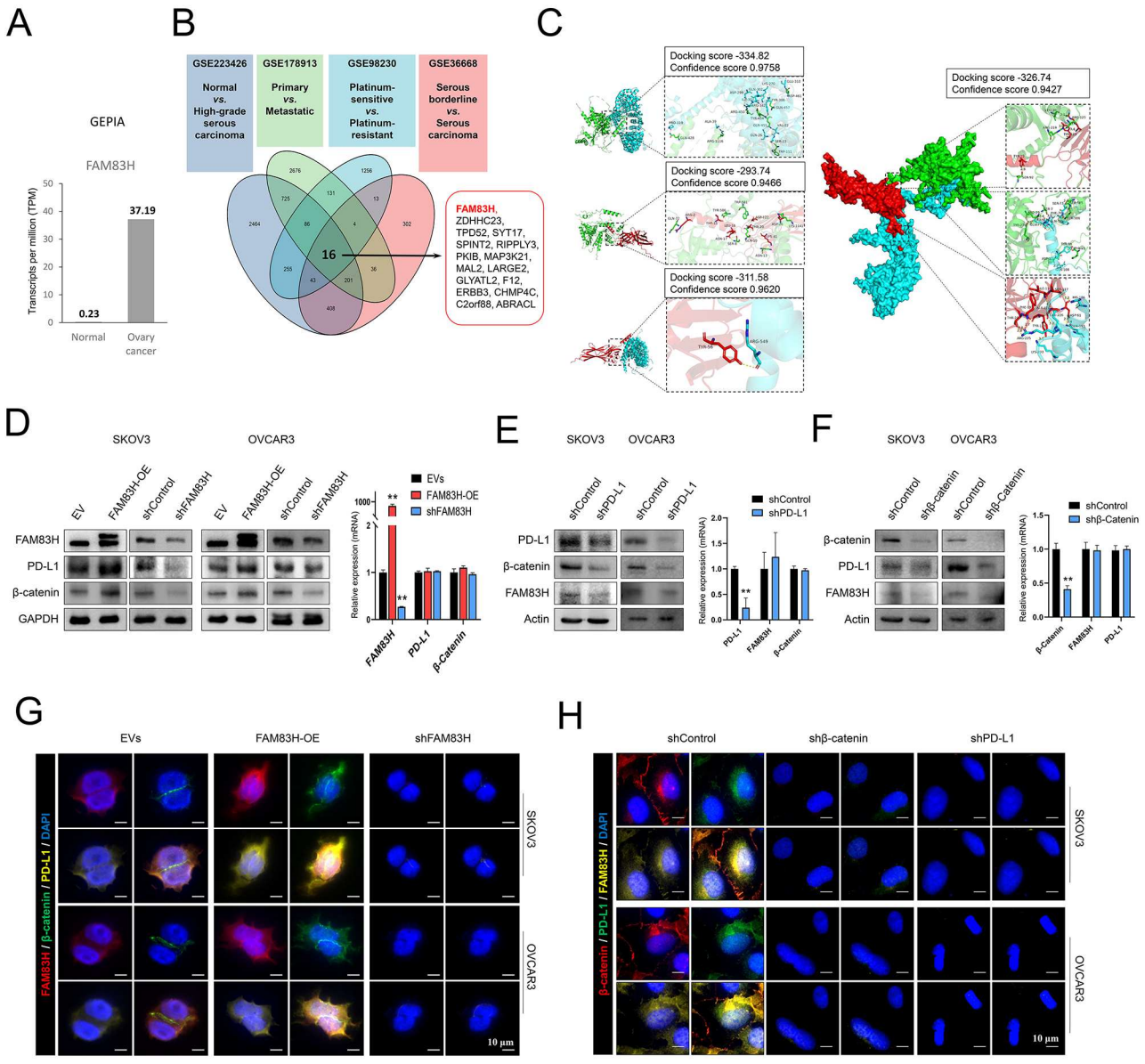
Abbreviations: 5y-OS, overall survival rate at five years; 10y-OS, overall survival rate at ten years; 5y-RFS, relapse-free survival rate at five years; 10y-RFS, relapse-free survival rate at ten years.

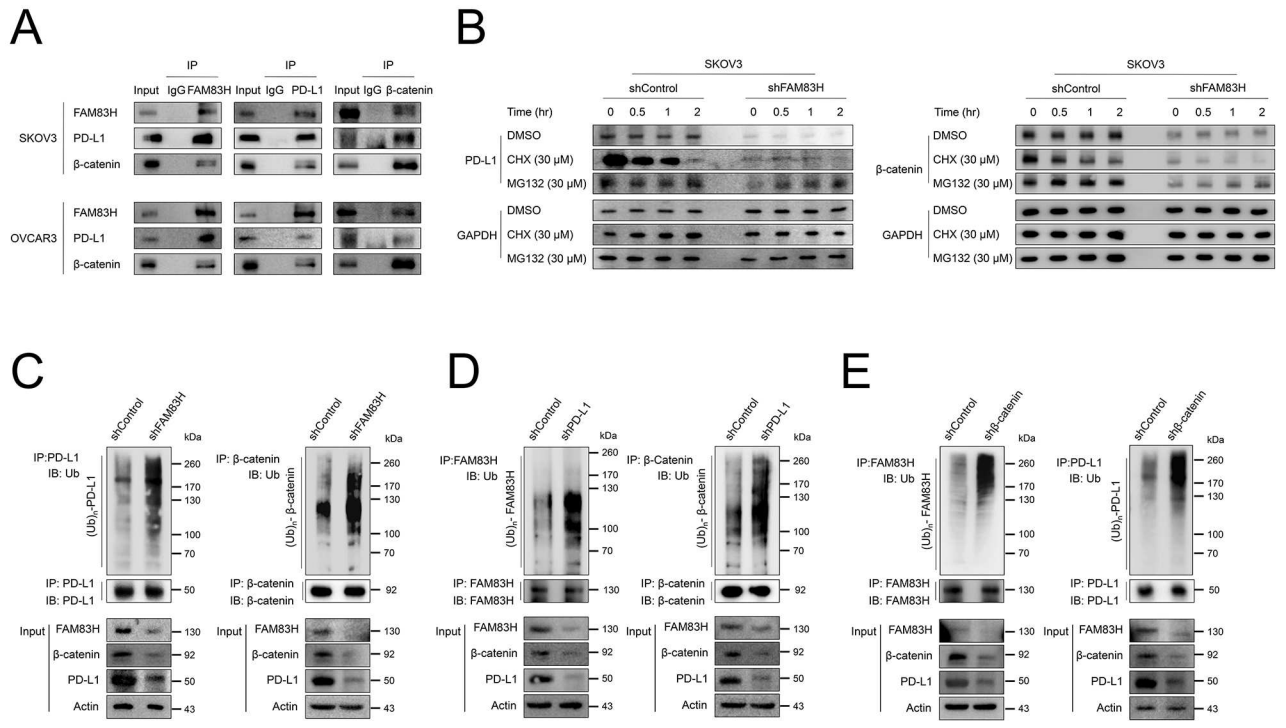


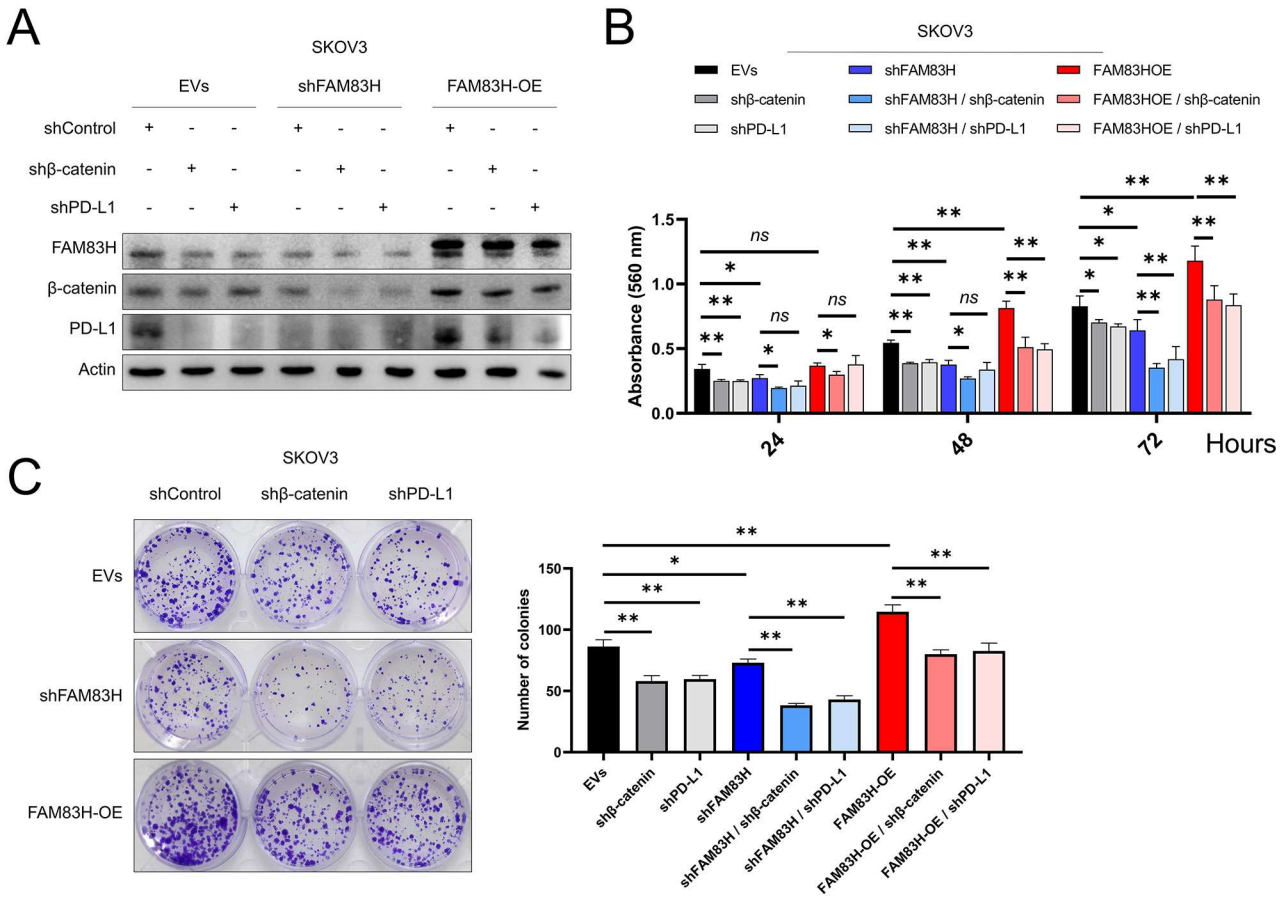
Variables	Cut-off	AUC	*P*
FAM83H	All	0.745	< 0.001
	≥ 9	0.710	< 0.001
PD-L1	All	0.731	< 0.001
	≥ 13	0.683	< 0.001
β-catenin	All	0.653	0.001
	≥ 11	0.673	< 0.001

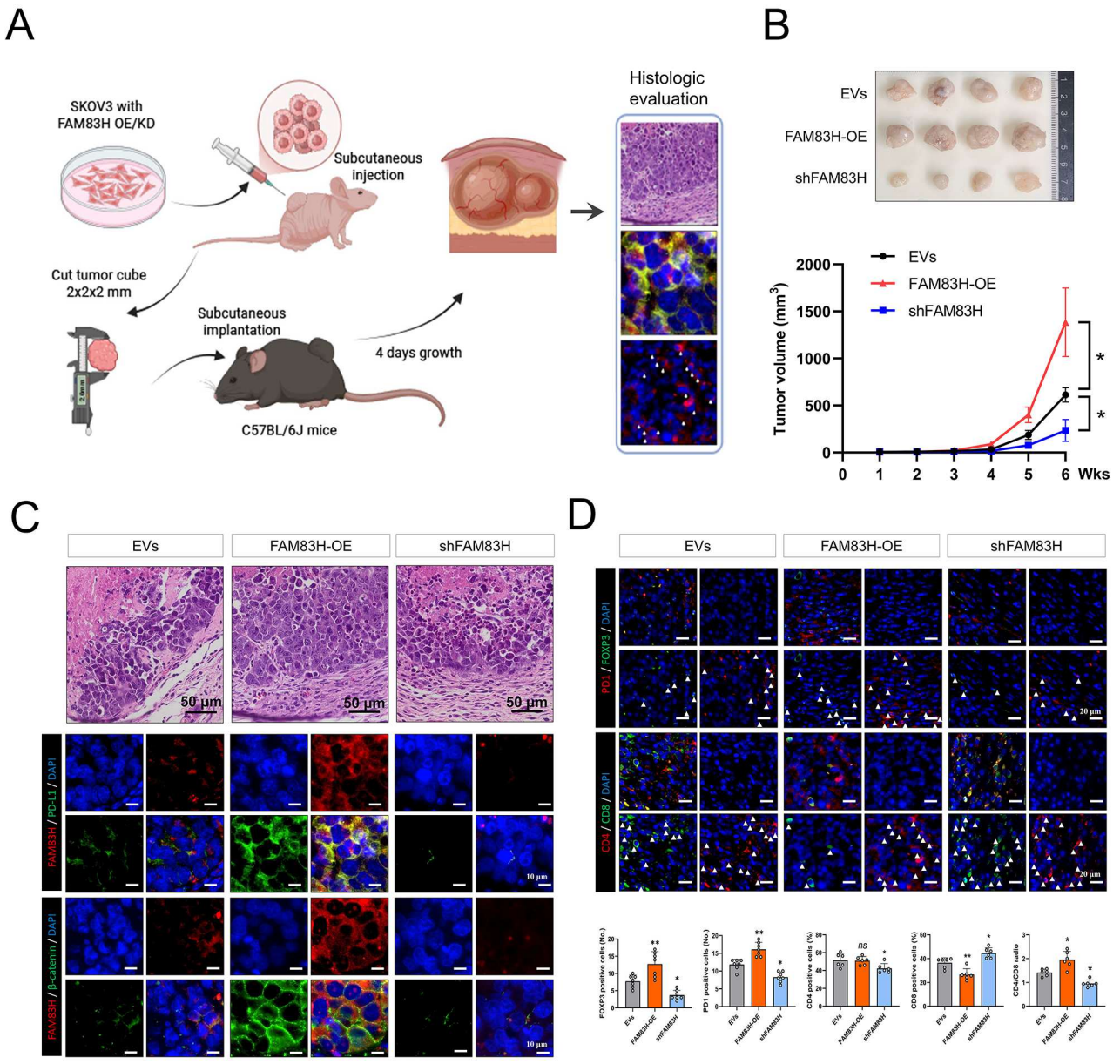

A
Log-rank, P = 0.003
FAM83H⁻, n=28
FAM83H⁺, n=49
Overall Survival
Duration (months)
Log-rank, P = 0.049
PD-L1⁻, n=26
PD-L1⁺, n=51
Overall Survival
Duration (months)
Log-rank, P = 0.006
β-catenin⁻, n=27
β-catenin⁺, n=50
Overall Survival
Duration (months)
Log-rank, P = 0.013
FAM83H⁻, n=28
FAM83H⁺, n=49
Relapse-free Survival
Duration (months)
Log-rank, P = 0.273
PD-L1⁻, n=26
PD-L1⁺, n=51
Relapse-free Survival
Duration (months)
Log-rank, P = 0.055
β-catenin⁻, n=27
β-catenin⁺, n=50
Relapse-free Survival
Duration (months)
B
Log-rank, P = 0.015
FAM83H⁻, n=26
FAM83H⁺, n=8
Overall Survival
Duration (months)
Log-rank, P = 0.064
PD-L1⁻, n=22
PD-L1⁺, n=12
Overall Survival
Duration (months)
Log-rank, P = 0.198
β-catenin⁻, n=22
β-catenin⁺, n=12
Overall Survival
Duration (months)
Log-rank, P = 0.013
FAM83H⁻, n=26
FAM83H⁺, n=8
Relapse-free Survival
Duration (months)
Log-rank, P = 0.048
PD-L1⁻, n=22
PD-L1⁺, n=12
Relapse-free Survival
Duration (months)
Log-rank, P = 0.129
β-catenin⁻, n=22
β-catenin⁺, n=12
Relapse-free Survival
Duration (months)


A
Log-rank, overall P < 0.001
Overall Survival
Score 0, n=37
Score 1, n=39
Score 2, n=41
Score 3, n=33
P = 0.300
P = 0.014
P = 0.005
Duration (months)
Log-rank, overall P = 0.001
Relapse-free Survival
Score 0, n=37
Score 1, n=39
Score 2, n=41
Score 3, n=33
P = 0.159
P = 0.156
P < 0.001
Duration (months)
B
Log-rank, P < 0.001
Overall Survival
Score 0 and 1, n=76
Score 2 and 3, n=74
Duration (months)
Log-rank, P < 0.001
Relapse-free Survival
Score 0 and 1, n=76
Score 2 and 3, n=74
Duration (months)
C
Log-rank, P = 0.020
Overall Survival
Score 0 and 1, n=12
Score 2 and 3, n=9
Duration (months)
Log-rank, P = 0.025
Relapse-free Survival
Score 0 and 1, n=12
Score 2 and 3, n=9
Duration (months)
D
Log-rank, P < 0.001
Overall Survival
Score 0 and 1, n=25
Score 2 and 3, n=52
Duration (months)
Log-rank, P = 0.156
Relapse-free Survival
Score 0 and 1, n=25
Score 2 and 3, n=52
Duration (months)
E
Log-rank, P = 0.006
Overall Survival
Score 0 and 1, n=24
Score 2 and 3, n=10
Duration (months)
Log-rank, P = 0.002
Relapse-free Survival
Score 0 and 1, n=24
Score 2 and 3, n=10
Duration (months)


A
GEPIA
FAM83H
Transcripts per million (TPM)
0.23
37.19
Normal
Ovary cancer
B
GSE223426
Normal vs. High-grade serous carcinoma
GSE178913
Primary vs. Metastatic
GSE98230
Platinum-sensitive vs. Platinum-resistant
GSE36668
Serous borderline vs. Serous carcinoma
16
FAM83H, ZDHHC23, TPD52, SYT17, SPINT2, RIPPLY3, PKIB, MAP3K21, MAL2, LARGE2, GLYATL2, F12, ERBB3, CHMP4C, C2orf88, ABRACL
C
Docking score -334.82
Confidence score 0.9758
Docking score -293.74
Confidence score 0.9466
Docking score -311.58
Confidence score 0.9620
Docking score -326.74
Confidence score 0.9427
D
SKOV3
OVCAR3
EV
FAM83H-OE
shControl
shFAM83H
FAM83H
PD-L1
β-catenin
GAPDH
EVs
FAM83H-OE
shFAM83H
Relative expression (mRNA)
FAM83H
PD-L1
β-Catenin
E
SKOV3
OVCAR3
shControl
shPD-L1
PD-L1
β-catenin
FAM83H
Actin
shControl
shPD-L1
Relative expression (mRNA)
PD-L1
FAM83H
β-Catenin
F
SKOV3
OVCAR3
shControl
shβ-catenin
β-catenin
PD-L1
FAM83H
Actin
shControl
shβ-Catenin
Relative expression (mRNA)
β-Catenin
FAM83H
PD-L1
G
EVs
FAM83H-OE
shFAM83H
FAM83H / β-catenin / PD-L1 / DAPI
SKOV3
OVCAR3
10 μm
H
shControl
shβ-catenin
shPD-L1
β-catenin / PD-L1 / FAM83H / DAPI
SKOV3
OVCAR3
10 μm


A
IP
Input IgG FAM83H Input IgG PD-L1 Input IgG β-catenin
SKOV3
FAM83H
PD-L1
β-catenin
OVCAR3
FAM83H
PD-L1
β-catenin
B
SKOV3
shControl
shFAM83H
Time (hr)
0 0.5 1 2 0 0.5 1 2
PD-L1
DMSO
CHX (30 μM)
MG132 (30 μM)
GAPDH
DMSO
CHX (30 μM)
MG132 (30 μM)
SKOV3
shControl
shFAM83H
Time (hr)
0 0.5 1 2 0 0.5 1 2
β-catenin
DMSO
CHX (30 μM)
MG132 (30 μM)
GAPDH
DMSO
CHX (30 μM)
MG132 (30 μM)
C
shControl
shFAM83H
kDa
IP:PD-L1
IB: Ub
(Ub)n-PD-L1
260
170
130
100
70
IP: PD-L1
IB: PD-L1
50
Input
FAM83H
β-catenin
PD-L1
Actin
130
92
50
43
shControl
shFAM83H
kDa
IP: β-catenin
IB: Ub
(Ub)n-β-catenin
260
170
130
100
70
IP: β-catenin
IB: β-catenin
92
Input
FAM83H
β-catenin
PD-L1
Actin
130
92
50
43
D
shControl
shPD-L1
kDa
IP:FAM83H
IB: Ub
(Ub)n-FAM83H
260
170
130
100
70
IP: FAM83H
IB: FAM83H
130
Input
FAM83H
β-catenin
PD-L1
Actin
130
92
50
43
shControl
shPD-L1
kDa
IP: β-Catenin
IB: Ub
(Ub)n-β-catenin
260
170
130
100
70
IP: β-catenin
IB: β-catenin
92
Input
FAM83H
β-catenin
PD-L1
Actin
130
92
50
43
E
shControl
shβ-catenin
kDa
IP:FAM83H
IB: Ub
(Ub)n-FAM83H
260
170
130
100
70
IP: FAM83H
IB: FAM83H
130
Input
FAM83H
β-catenin
PD-L1
Actin
130
92
50
43
shControl
shβ-catenin
kDa
IP:PD-L1
IB: Ub
(Ub)n-PD-L1
260
170
130
100
70
IP: PD-L1
IB: PD-L1
50
Input
FAM83H
β-catenin
PD-L1
Actin
130
92
50
43


A
SKOV3
EVs
shFAM83H
FAM83H-OE
shControl
shβ-catenin
shPD-L1
FAM83H
β-catenin
PD-L1
Actin
B
SKOV3
EVs
shFAM83H
FAM83HOE
shβ-catenin
shFAM83H / shβ-catenin
FAM83HOE / shβ-catenin
shPD-L1
shFAM83H / shPD-L1
FAM83HOE / shPD-L1
Absorbance (560 nm)
Hours
24
48
72
C
SKOV3
shControl
shβ-catenin
shPD-L1
EVs
shFAM83H
FAM83H-OE
Number of colonies
EVs
shβ-catenin
shPD-L1
shFAM83H
shFAM83H / shβ-catenin
shFAM83H / shPD-L1
FAM83H-OE
FAM83H-OE / shβ-catenin
FAM83H-OE / shPD-L1


A
SKOV3 with FAM83H OE/KD
Subcutaneous injection
Histologic evaluation
Cut tumor cube 2x2x2 mm
Subcutaneous implantation
4 days growth
C57BL/6J mice
B
EVs
FAM83H-OE
shFAM83H
Tumor volume (mm3)
Wks
C
EVs
FAM83H-OE
shFAM83H
50 μm
FAM83H / PD-L1 / DAPI
FAM83H / β-catenin / DAPI
10 μm
D
EVs
FAM83H-OE
shFAM83H
PD1 / FOXP3 / DAPI
CD4 / CD8 / DAPI
20 μm
FOXP3 positive cells (No.)
PD1 positive cells (No.)
CD4 positive cells (%)
CD8 positive cells (%)
CD4/CD8 radio
ns

Supplementary Files

This is a list of supplementary files associated with this preprint. Click to download.

- SupplementaryTables.docx